A Bayesian Belief Network Model for the Risk Assessment and Management of Premature Screen-Out during Hydraulic Fracturing

Enrico Zio, Maryam Mustafayeva, Andrea Montanaro

Version of Record: https://www.sciencedirect.com/science/article/pii/S0951832021005913
Manuscript_2615a38a14e86404f43e4427861c4a65

A Bayesian Belief Network Model for the Risk Assessment and Management of Premature Screen-Out during Hydraulic Fracturing

Enrico Zio[1], Maryam Mustafayeva[2] and Andrea Montanaro[3]

[1]Centre de Recherche sur les Risques et les Crises (CRC), MINES ParisTech/PSL Université Paris, Sophia Antipolis, France.

[1]Department of Energy, Politecnico di Milano, Milan, Italy.

[1]Eminent Scholar at the Department of Nuclear Engineering, Kyung Hee University, Seoul, South Korea.

[2]Department of Management, Economics and Industrial Engineering, Politecnico di Milano, Milan, Italy.

[3]Kwantis.

Corresponding authors: [1]enrico.zio@polimi.it

Abstract

Hydraulic fracturing is a well completion technique for Oil and Gas production enhancement in both conventional and unconventional reservoirs. However, it can result in the unfavorable consequence of the premature screen-out, which occurs due to the proppant bridging across the perforations or similar restricted flow areas.

The objective of this work is to propose a novel framework of analysis that enables to quantify the risk of screen-out occurrence, to identify the riskiest scenarios and to determine the best risk mitigation strategies. The premature screen-out problem is addressed within a Risk Management and Control Process, wherein the qualitative and quantitative assessments of the early screen-out risk are performed by a Features, Events and Processes Analysis structured with a Bayesian Belief Network. The BBN probabilities are subject to a thorough uncertainty and sensitivity analysis. Sensitivity analysis is performed by the Sobol's variance decomposition method and the identified most influential probabilities of the BBN are re-estimated in order to reduce the output uncertainty.

Finally, risk mitigation plans are formulated using risk importance measures to identify the riskiest scenarios and cost-benefit analysis to determine the optimal risk reduction actions

The developed framework has been applied to a case study of vertical wells.

Keywords: premature screen-out, risk assessment, Bayesian Belief Network, experts probability elicitation, Sobol's indices, robustness of Bayesian Networks, risk importance measures, scenario analysis

Nomenclature

A	Causal arcs
a	Lower limit of the Uniform and Gaussian Distributions
b	Upper limit of the Uniform and Gaussian Distributions
BBN(s)	Bayesian Belief Network(s)
$Comp\left(X_{pi} = x_{pi}^{ji}\right)$	Compatible parental configuration for the *jth* state of the *ith* probability
CPT(s)	Conditional Probability Table(s)
D	Total variance of the model output
DAG	Directed Acyclic Graph
EBBN	Elicitation method for the BBN
$\mathbb{E}[\mathcal{U}]$	Expected disutility
FEP	Features, Events and Processes
f_0	Average of the model output variance
f_i	Function of the individual effects of the *ith* input parameter
f_{ij}	Function of the interaction effects of the *ith* and *jth* input parameters
I_{ind}, I_{joint}	Individual and joint influence factors
NWBF	Near-Wellbore Friction
$p(s_i)$	Marginal probability of the state of the *ith* component
$p(s_i \mid S_I)$	Conditional probability of the state of the *ith* component given the combination of the states of its parents S_I
$p(\mathbb{S})$	Probability of scenario $\mathbb{S}$
$p(X_i)$	Probability of the input parameter
$pa(X_c)$	The set of parent nodes of X_c
RAW	Risk Achievement Worth
RIM	Risk Importance Measures
RRW	Risk Reduction Worth
RS	Risk Share
s	Path vector
$\overline{\mathbb{S}}$	Scenario exclusion
S_i	First-order Sobol's Sensitivity index of the *ith* input parameter
ST_i	Total-effect Sobol's Sensitivity index of the *ith* input parameter
T_r	Typical distribution
$\mathcal{U}[X_u(s_{I(u)})]$	Disutility function for all combinations of states of the parents $s_{I(u)}$
x	Random variable
X_{max}	Highest-ordered state
X_{min}	Lowest-ordered state
$X_{pi} \in pa(X_c)$	*ith* parent node of the set of parent nodes of a child node X_c
X_c	Child node
w_i	Relative influence weight of the *ith* parent node
WSA	Weighted Sum Algorithm

Greek letter parameters

$\alpha_{x_{pi}}$	Weighting Factor of the *ith* parent node
β_{x_c}	Weighting Factor of a child node X_c
$\gamma_{x_c x_{pi}}$	Influence weight parameter of the *ith* parent node and a child node X_c
μ	Mean value
σ	Standard deviation

1. Introduction

Hydraulic fracturing is a widespread well completion technique for Oil and Gas production enhancement in both conventional and unconventional reservoirs. It amounts to the injection of fracking fluid, i.e. the pressurized liquid, into a wellbore in order to create fractures in the rock formations and, then, keeping them open using proppants, i.e. solid materials. The design of this technique depends heavily on the mechanical properties of the rock formation, the petrophysical properties of the reservoirs and the nature of the fracturing process. The reliability of the operation relies on the data inferred from the measurement logs, laboratory analyses and core sample tests. A low quality of the data may cause failures and result in the most unfavorable consequence of premature screen-out [5].

The screen-out is a condition due to the proppant bridging across the perforations or similar restricted flow area, i.e. inside near-fractures, that leads to a rapid increase in the pump pressure, as in the example of Figure 1. This situation obstacles the hydraulic fracturing and leads to the loss of working days and costs for the remedial operations [5]. Because of its detrimental effects, predicting the risk of occurrence of the screen-out is very important.

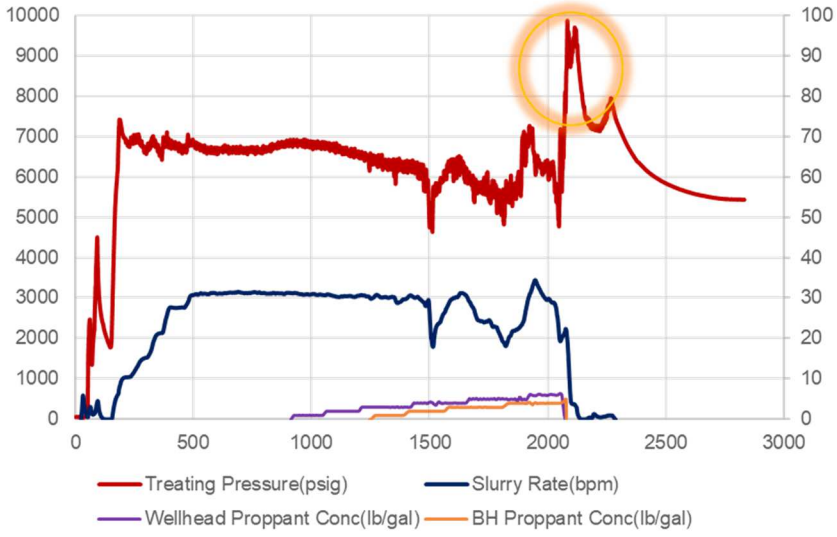

Figure 1 Premature Screen-Out conditions (internal, non disclosable communication Kwantis)

Currently, the potential for screen-out occurrence can be assessed by hydraulic fracturing calibration tests, such as the Step Rate Tests and MiniFracs. Specifically, the Step Rate Tests are fluid injection tests carried out before the main fracturing job, in order to gather important information about the fracture pressure and determine the entry friction losses through perforations and near-wellbore area. The excessive friction losses obtained from the tests indicate the presence of tortuosity and multiple fractures in the vicinity of a wellbore, which may result in the early screen-out. The Nolte-Smith method can, then, be used to provide a log-log plot that describes the expected pressure response from the formation

during pumping in order to predict the fracture propagation behavior and the tendency of hydraulic fracturing to screen-out. This approach is based on different fracture geometry models and implies specific assumptions, which can deviate from the real conditions [6].

The MiniFrac is an injection test of the fracturing fluid, which aims to evaluate fracture and fluid behavior. The MiniFrac fall off analysis with the G-Function Plot Analysis is a pressure decline analysis that provides a more accurate measure of the fracture behavior, and identifies such coefficients as fluid leak-off and fluid efficiency: these two parameters may indicate the presence of natural fractures or high permeability zones, which are the possible root causes of the premature screen-out [6].

It is worth noting, that these tests have the following deficiencies:

1. They give only the signs of occurrence of the screen-out.
2. Analysis results are obtained only in real time – thus, it is not possible to predict the occurrence of the screen-out in advance, before carrying out the treatment.
3. Potential primary causes of screen-out are identified during different stages of the job execution – consequently, there is no comprehensive model that identifies different scenarios of the premature screen-out at the same time.

In this work, the premature screen-out problem has been addressed within a novel and complete framework of Risk Management and Control Process (RMCP). Traditionally, the RMCP within the Oil and Gas projects consists of qualitative assessment of the potential risks by performing such methods as Failure Mode and Effect Analysis (FMEA), Hazard Operability (HAZOP) analysis, and of quantitative assessment by implementing Decision Tree Analysis (DTA) and Event Tree Analysis (ETA). Then, the level of risks is prioritized using the Risk Matrix. The risks are evaluated in terms of Expected Monetary Value (EMV) [2].

In this work, the hazards contributing to the early screen-out failure have been identified by Features, Events and Processes (FEP) analysis. The quantitative part of the risk assessment is based on a Bayesian Belief Network (BBN), a descriptive and quantitative probabilistic graphical model. The probabilities that feed the model have been assessed using different expert elicitation methods, namely the Weighted Sum Algorithm (WSA), the elicitation method for BBN, the log-likelihood method. The latter method has provided the most satisfactory results for the big matrices of the Conditional Probability Tables (CPT) of the BBN and has been used to provide the input for the risk quantification.

The robustness of the BBN model and its sensitivity to the input probabilities have been evaluated through extensive uncertainty and sensitivity analyses. The outcome of the uncertainty analysis has shown that the model is robust to small variations in its input probabilities. The influence of the input parameters variability on the output distribution has been assessed by the Sobol's variance decomposition method. The most sensitive probabilities have been re-evaluated using historical data and experts judgement, in order to reduce the output uncertainty.

Finally, the riskiest scenarios have been identified by introducing risk importance measures. The best risk mitigation plans have been identified by cost-benefit analysis.

The remainder of the paper is structured as follows (Figure 2):

- Section 2 formulates the risk assessment by describing the FEP analysis of Hydraulic Fracturing and defines the methodological framework based on BBN.
- Section 3 unfolds different methods for the estimation of the probabilities of the BBN model.
- Section 4 illustrates the sensitivity and uncertainty analyses.
- Section 5 describes the risk importance measures analysis and the cost-benefit analysis.
- Section 6 presents the results of the analyses carried out.

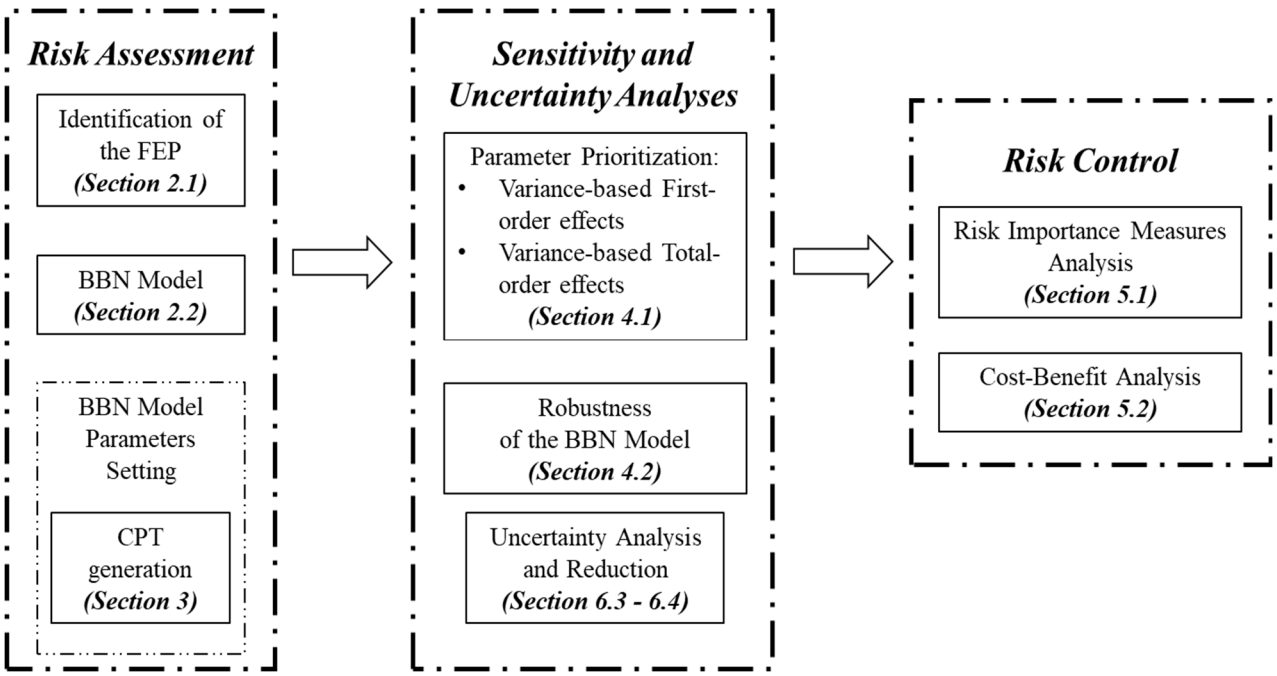

Figure 2 Framework of the Risk Management and Control Process for Premature Screen-Out failure

2. Risk Assessment

Risk assessment is a part of the Risk Management and Control Process (Figure 3), which provides a structured process for the risk identification, risk analysis and risk evaluation. Risk assessment consists of two parts [1]:

1. Qualitative part: the objective of this part is to identify all potential sources of danger, which can lead to substantial consequences.

2. Quantitative part: the objective of this part is to evaluate possible accident scenarios and estimate failure probabilities.

In this work, the hazards contributing to the early screen-out failure are identified by FEP analysis, whereas the quantitative part of the risk assessment is based on a Bayesian Belief Network.

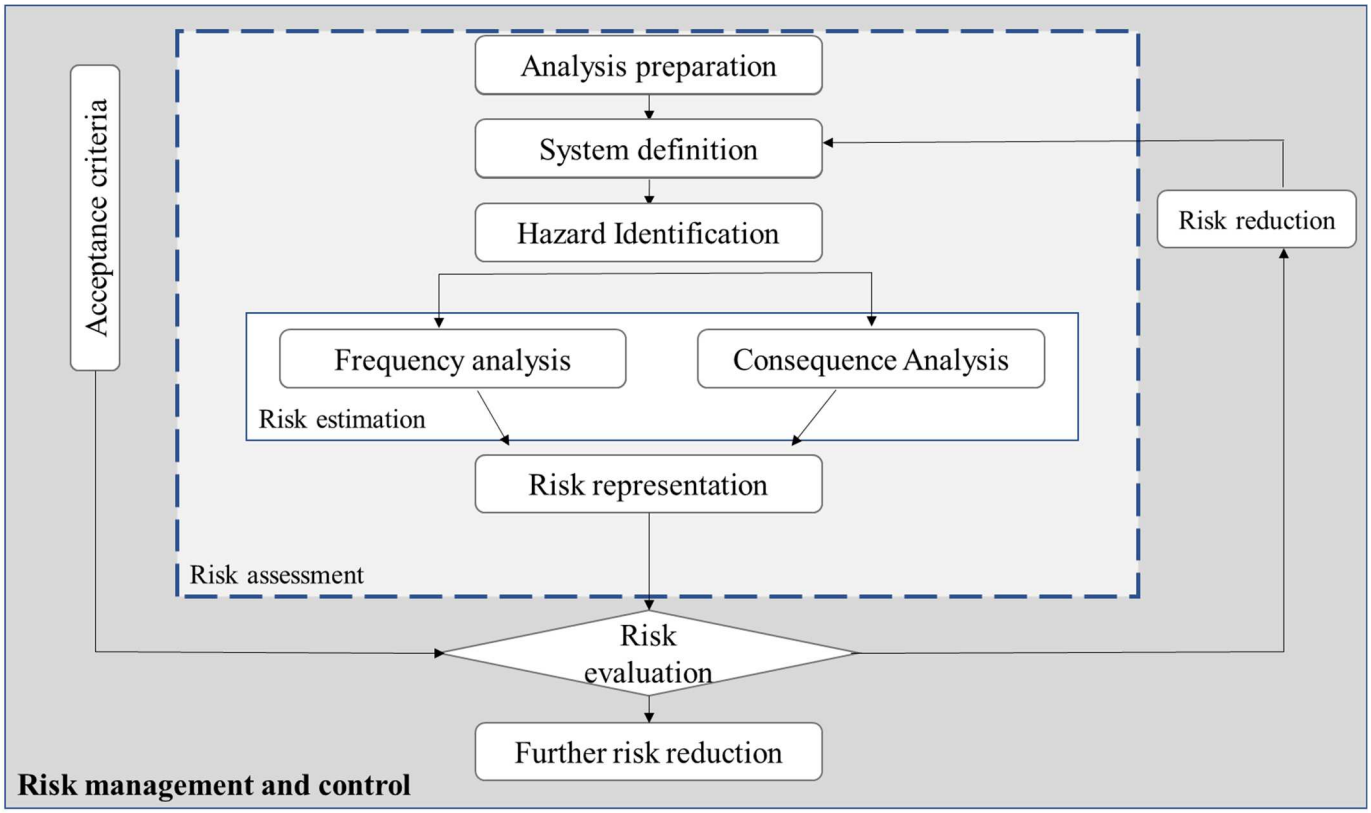

Figure 3 Risk Management and Control Process

2.1 Identification of the Features, Events and Processes

FEP analysis is a structured method, which aims to identify the factors affecting the system performance and the important interactions among these factors. The literature shows that FEP analysis is quite adequate for the analysis of complex models. The condition of the FEP elements identified in the analysis can be represented in multiple states, whose possible scenarios of evolutions in the system can be described and probabilistically evaluated by means of BBN [10].

FEP analysis can be performed in either two ways: bottom-up or top-down. In the bottom-up approach, the FEP are assigned the initial state values and the evolution of the system is assessed as a result of the evolution of FEP interactions. In the top-down approach, the process of analysis proceeds to identify the combinations (scenarios) of FEP that lead the system to failure [10].

In the context of Hydraulic Fracturing, the components of the FEP are classified in terms of the main geological features, key events and main processes occurring during the fracturing job execution [4], where:

1. “Features” characterize the static system of the environment.
2. “Events” represent changes in the system, as a result of the fracturing operation or due to the natural environment.
3. “Processes” describe the way the system and conditions change over time.

In this work, the top-down approach has been considered to explicitly identify those FEP that can lead to early screen-out (Table 1). In particular, company experts have:

1. Identified the potential root causes of early screen-out coming from the static system of the environment, i.e. features of the rock formation.
2. Determined the hazardous events possibly occurring as a result of the fracturing process and geological conditions of the formation.
3. Defined the parameters of the hydraulic fracturing job execution, whose measures are relevant in the occurrence of the root causes of early screen-out.

Table 1

FEP for the Premature Screen-Out

Type	Node	States		Units
Features	High Permeability Zones	No	Yes	-
	Natural Fractures	No	Yes	-
Events	Degree of Tortuosity	Low	High	-
	Multiple Fractures	No	Yes	-
	Excessive Leak-Off	No	Yes	-
	Poor Erosion	No	Yes	-
	Reduced Fracture Geometry	No	Yes	-
Processes	Perforation Friction	Low	High	Psi
	Near-Wellbore Friction	Low	High	Psi
	Closure Gradient	Low	High	Psi/ft
	Fluid Viscosity	Sufficient	Insufficient	cP
	Fluid Efficiency	High	Low	%
	Max Treating Pressure	Low	High	Psi
	Pad Volume	Sufficient	Insufficient	%
	Pump Proppant Slugs	No	Yes	-

2.1.1 Features

There exist several aspects affecting a proppant transportation, among which the geological conditions of the formation and the reservoir properties of the rock are of main concern.

The natural fractures in the formation are considered to be among the major causes for screen-out. During the hydraulic fracturing operation, the induced fractures tend to connect to the pre-existing cracks in the formation, since they are structurally the weakest points. As a result, a significant portion of the injected fluid is lost in such fissures, reducing the fluid efficiency and leading to a narrower fracture width (refer to Figure 4) [5]. Apart from the natural fractures effect on the hydraulic fracturing, the situation is worsened by the difficulty of defining the location of such fissures during the reservoir modelling that guides the hydraulic fracturing operation.

Another cause of screen-out coming from the formation properties, is high permeability zones. In the presence of the high permeability zones, the fracturing fluid is not able to build a filter cake, i.e. a layer formed by solid particles, on the fracture face to control the fluid loss [5]. This leads to a high leak-off, resulting in a low efficiency of the fracturing fluid. The premature screen-out, then, occurs because a proppant dehydrates too quickly and packs inside the fracture, impeding the fluid to flow towards the tip of the fracture.

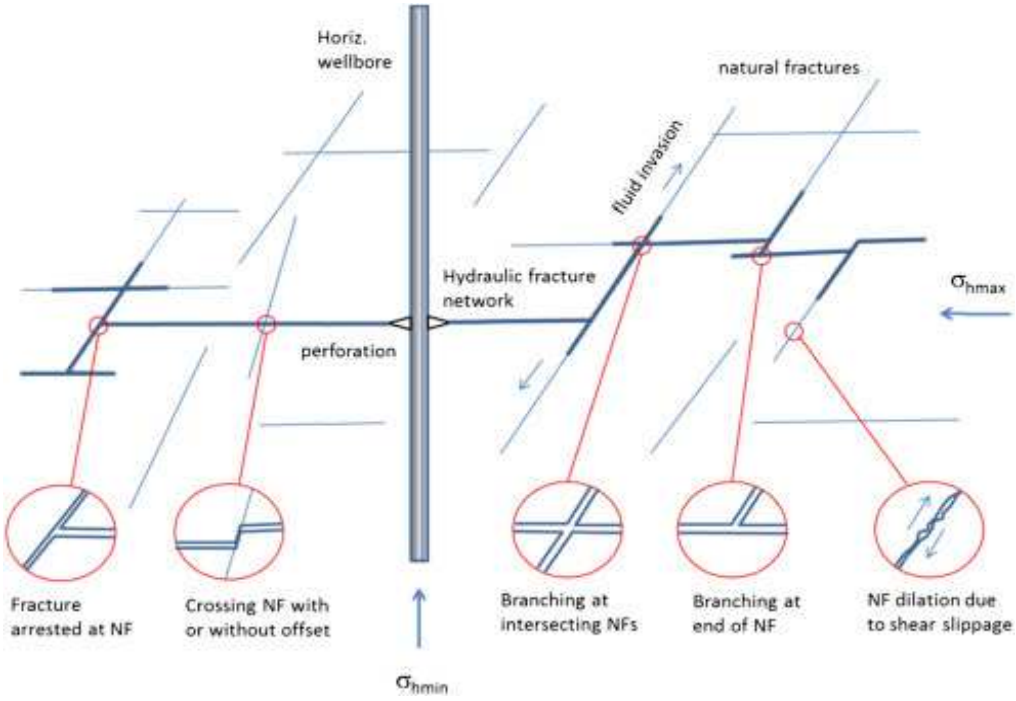

Figure 4 Impact of pre-existing natural fractures on the induced fractures [11]

2.1.2 Events

The near-wellbore geometry effects, such as tortuosity and multiple fractures, are also relevant for the success of the fracturing treatment. The tortuosity is a convoluted pathway between the perforations and the main body of the fracture, formed as a result of a misalignment of the wellbore and stress fields. The fractures generally propagate in the direction of the maximum horizontal stress and perpendicular to the minimum horizontal stress. When a significant contrast between these in-situ stresses appears, the fracture makes a dramatic change in the orientation of the fracture propagation, thus resulting in a reduced fracture geometry. The oil and gas industry considers tortuosity to be one of the biggest causes of the premature screen-outs that have occurred worldwide [5] (refer to Figure 5).

The orientation differences between the perforation and the maximum principle stress may result in multiple fractures. Multiple fractures are fractures which grow simultaneously from a wellbore. They can have a considerable impact on the obtained fracture geometry. When the fluid enters multiple fractures, the fluid volume and proppant are shared by these fractures and, as a result, a narrower fracture is obtained [6]. Furthermore, the widths of the individual multiple fractures are smaller than the width of a single fracture, possibly giving rise to screen-out.

Another predominant factor that affects fracture geometry is the pad, which is a volume of the clean fluid, determined as the percentage of the total slurry (the fluid plus proppant) volume varying from 20% to 40%. This fluid is pumped first in order to create the fracture [6]. Thus, it is important to maintain a sufficient pad volume in order to obtain an effective fracture volume to accommodate a proppant.

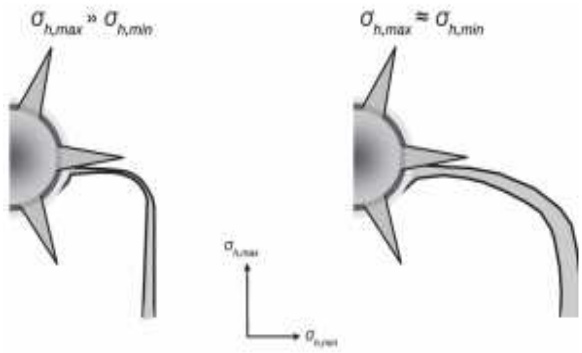

Figure 5 The illustration of the effects of horizontal stress contrast on tortuosity [6]

2.1.3 Processes

Obtaining an accurate description of the fracture propagation process and the resulting fracture geometry is complex and difficult. The calibration tests, such as the Step Rate Tests and MiniFracs, which are used for the above-mentioned purposes, have been discussed in Section 1. In this section a particular attention is drawn to the physical components of the test processes, which determine the Features and Events.

High Near-wellbore Friction (NWBF) losses are evidence of tortuosity and multiple fractures. The NWBF loss is the frictional pressure drop along the flow path between the wellbore and the main body of the fracture, caused by the effects of tortuosity and perforation friction. Perforation friction is the pressure loss that occurs as the fracturing fluid passes through the restricted flow area of the perforations. A poor alignment among the perforations, wellbore and the main body of the fracture, as well as a creation and propagation of multiple fractures, cause a poor wellbore and fracture communication, resulting in excessive pressures. In addition, these friction losses make the treating pressure higher than it would normally be [6].

The value of the bottom-hole treating pressure minus the closure pressure is the key parameter in determining the geometry and the leak-off characteristics of the fracture. The leak-off coefficient and the fluid efficiency parameter are reversely related to each other. The fluid efficiency describes the ability of the fluid to create fractures. It is the ratio between the volume of the fracture to the total volume of the fluid injected into the fracture. Thus, the greater the fluid efficiency, the greater the volume of the fracture and the less the fluid leak-off [6].

Another key parameter, which affects the fracturing treatment, is fluid viscosity. More precisely, fluid viscosity is the factor that affects the net pressure inside the fracture (and, thus, its width) and controls the fluid's ability to transport proppants. A sufficient fluid viscosity within a range suitable for the treatment is required to get a good proppant transport and an adequate fracture width [6].

2.2 Bayesian Belief Network Model

Bayesian Belief Network is a probabilistic graphical model that represents conditional dependencies between random variables through a Directed Acyclic Graph (DAG). The quantification of the model amounts to computing the posterior probabilities of any set of nodes and propagate evidences from any part of the network, even in case of uncertain or incomplete information. BBN can be applied for modelling complex systems and processes with multiple scenarios, and executing forward, backward and intercausal inferences [9].

In BNs, the model $G = (V, A)$ is made of a set $V = \{1, \dots, n\}$ of nodes representing random variables (which, in this work, correspond to the FEP) and a set of directed links $A = \{(i,j) | i,j \in \mathrm{V}, i \neq j\}$ connecting the nodes and representing the causal dependencies between the random variables. Specifically, link $(j,i) \in A$ represents the fact that the output of node i depends on the value of the random variable in node j. The nodes $I(i) = \{j \in V | (j,i) \in A\}$ are the parents of i, and i is the child of each of its parents [9]. Figure 6 represents the BBN model developed for the premature screen-out. The nodes, shown as circles, correspond to the FEP and the arcs indicate the causal dependencies between them. For instance, the Natural Fractures (j_{NF}) and High Permeability Zones (j_{HPZ}) are the parents of the Excessive Leak-Off (i_{EL}), and Excessive Leak-Off is the child of Natural Fractures and High Permeability Zones (see Figure 6).

Each node $i \in V$ is associated with a random variable with at least two discrete states $s_i \in S_i$, where a given state s_i corresponds to a range of values representing the state of the i-th element of the FEP [9]. Specifically in this work, each node of the BBN is associated with two states: low ("success")-order state and high ("failure")-order state. The former represents the physical state of the node that is such to not violate the performance of its child node; the latter is the state of the node for which the performance of its child node is violated, thus leading to its "failure". For example, Natural Fractures has "No" (NF_{No}) and "Yes" (NF_{Yes}) states (see Figure 6): the "failure" (NF_{Yes}) state of the node Natural Fractures leads to the "Yes" (failure) state of its child nodes "Excessive Leak-Off" (EL_{Yes}) and "Reduced Fracture Geometry" (RFG_{Yes}).

A path $s = (s_1, \dots, s_n)$ is a vector, which associates a state $s_i \in S_i$ with each component $i \in V$, whose joint probability distribution is [9]:

$$p(s) = \prod_{i=1}^{n} p\left(s_i \left| S_{I(i)}\right.\right) \quad (1)$$

where:

- the state probabilities of variables with no parents ($S_{I(i)} = \emptyset$) are given by the marginal probabilities $p(s_i) = \mathbb{P}(X_i = s_i)$.

- the probabilities of the states of variables with parents are given by the conditional probabilities $p(s_i\,|S_I) = \mathbb{P}(X_i = s_i|X_j = s_j, j \in I_{(i)})$.

- $S_{I(i)}$ indicates the set of the states of the parents of *i*.

The size of the network grows linearly with the number of the random variables, whereas the joint distribution grows exponentially [9].

Figure 6 BBN for Premature Screen-Out

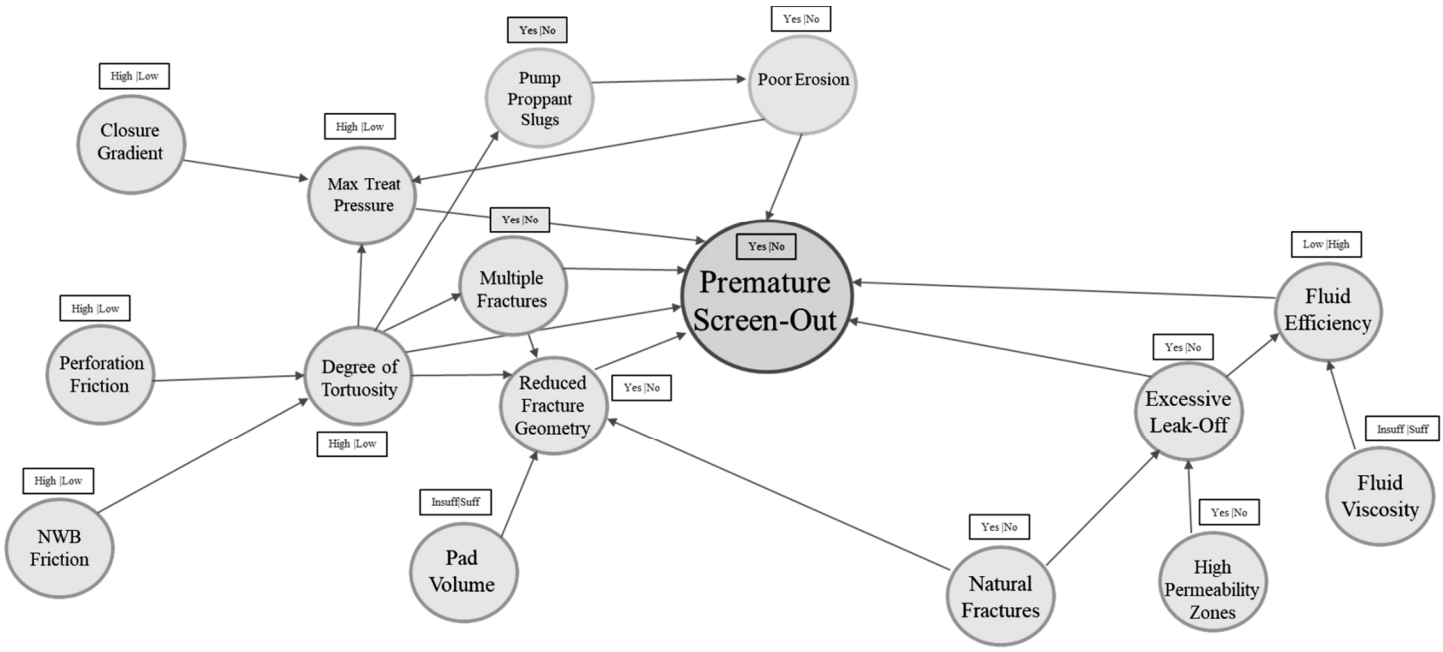

3. BBN Model parameters setting

The computation of the joint probability distribution requires an estimation of the marginal probabilities of the nodes with no parents and of the conditional probabilities of the child nodes dependent on their parent, as indicated in the BBN. In practice, there are two main methods for setting the parameters of the BBN [11]:

1. Maximum likelihood estimation.

2. Expert elicitation.

In this work, the conditional probabilities have been obtained by expert elicitation for the following reasons:

1. The only recorded data available represent the characteristics of the treatment design and the parameters of the hydraulic fracturing operation monitored by the engineers during the execution.

2. There are missing data regarding the changes in the environment, i.e. wellbore characteristics and reservoir properties, as a result of the preliminary fracturing test.

The marginal probabilities of the nodes with no parents have been directly assessed by the experts using a probability scale, whereas the conditional probabilities have been assessed using heuristic approaches of expert elicitation. No database/historical observations were used in the first evaluation to explore the probabilities.

The conditional probabilities have been organized in Conditional Probability Tables (CPTs), containing the probabilities of the states of the child nodes conditional on the states of the parent nodes. The size of the CPT grows exponentially with the number of parent nodes and their states and, in some practical cases, the number of probabilities to assess can grow up to hundreds or even thousands. Different methods have been proposed for generating CPT that would reduce the cognitive efforts of the experts in assessing the probabilities. In this work, the three methods, Weighted Sum Algorithm (WSA), Log-likelihood and Elicitation for BBN (EBBN), have been selected to generate the CPT for the following reasons [15]:

1. The experts are able to define both the influencing weights of the parent nodes on the child nodes and some specific probabilities.

2. These methods address compatible (likely) parental configurations for child nodes, such as Max Treating Pressure, Fluid Efficiency, Unexpected Leak-Off, Degree of Tortuosity, and Premature Screen-Out. This means that low (high) - ordered states of the parent nodes of these child nodes are likely to co-occur with low (high) - ordered states of other parent nodes, as illustrated in the example in Table 2.

3. These methods are suited for medium and large size matrices.

4. The methods are simple, flexible and time-saving.

Weighted Sum Algorithm is based on the concept of a compatible parental configuration and the assignment of a weight of influence of the parent nodes on the child node. The compatible parental configuration refers to those combinations of states of parent nodes which are more likely to co-exist [14], for example, the combination of "High Perforation Friction" and "High NWB Friction".

Table 2

Compatible parental configuration for the node "Degree of Tortuosity"

Parent node	State	Compatible parental configuration for Degree of Tortuosity
Perforation Friction	High	High NWB Friction
	Low	Low NWB Friction
NWB Friction	High	High Perforation Friction
	Low	Low Perforation Friction

Log-Likelihood method is based on the indirect assessment of probabilities by defining the influence weights of each state of the parent nodes on the child node, the states of a child node itself and their probabilities.

Elicitation for BBN method is based on a piecewise linear interpolation of the rank of states of the parent nodes. The rank of states of the parent nodes should be ordered with respect to the negative/positive influence on the states of the child node, in order to determine the CPT. The EBBN method requires experts only to assign as many rows of the CPT as there are child states and one weight for each parent node [15].

The elicitation procedure and the calculation methods of the above-mentioned heuristic approaches are described in Appendix A.

4. Sensitivity and uncertainty analyses

The BBN model's probabilities represent the input uncertainty, which may be caused by the experts' subjective elicitation or by inaccurate or incomplete data. The input uncertainty, then, propagates through the BBN and leads to the uncertainty in the model output.

Sensitivity analysis applied to BBN allows examining the model behavior to reveal the relationship between the local (input) and global (output) dependence beliefs described in the network by the CPT. The final objective is to investigate how the uncertainty of the BBN outcome depends on the BBN input parameters. In particular, sensitivity analysis helps to identify the key uncertainty drivers so that the analysts may further optimize data collection and calibration efforts [18].

Uncertainty analysis, on the other hand, allows assessing the robustness of the BBN model by varying values of the BBN input parameters [24].

In addition, the sensitivity and uncertainty analyses help in evaluating the integrity of the BBN's model. The results of the sensitivity analysis guide on the re-adjustment or elimination of the model's nodes in case of misalignment with the system's expected behavior and sensitivity indices equal to 0. The uncertainty analysis gives an evaluation of the model behavior under variations and suggests model reconfiguration in case of unrealistic results [33].

4.1 Parameter Prioritization

In this work, the Sobol's Variance Decomposition Global Sensitivity Analysis method has been applied to identify the influential local beliefs of the BBN for premature screen-out. This technique is able to quantify the individual and interaction effects of the parameters on the BBN model output, and provides information about the order of the influence [16].

Take the BBN model under examination as described by an overall function $y = f(x)$, where x is a vector of d uncertain model inputs $\{x_1, x_2, \dots, x_d\}$ inside an n-dimensional black box and y is a scalar output. Under the conditions that the inputs are uniformly and independently distributed within the unite hypercube, i.e. $x_i \in [0,1]$ for $i = 1, \dots, d$, the model output function $y = f(x)$ can be uniquely decomposed into systematic functional components [16]:

$$f(x_1, \dots, x_k) = f_0 + \sum_{i=1}^{k} f_i(x_i) + \sum_{i<j} f_{ij}(x_i, x_j) + f_{12..k}(x_1, \dots x_k) \qquad (2)$$

where:

- f_0 is a constant that represents the expected value of the model output.
- f_i is a function of x_i that corresponds to individual effects.
- f_{ij} is a function of x_i and x_j that corresponds to interaction effects.
- $f_{12..k}(x_1, \dots x_k)$ is a function of all input variables that corresponds to their cooperative influence on the output function.

In order to estimate the Sobol's indeces the following integrals are to be computed [34]:

$$f_0 = \int_{\Omega^k} f(x)dx \qquad (3)$$

$$D_{i_1\ldots,i_s} = \int_0^1 \ldots \int_0^1 f^2_{i1,\ldots,is}(x_{i1,\ldots,}x_{is})dx_{i1},\ldots dx_{is} \qquad (4)$$

$$D = \sum_{s=1}^{N} \sum_{i_1<\ldots<i_s}^{N} D_{i_1\ldots,i_s} = \int_{\Omega^k} f^2(x)dx - f_0^2 \qquad (5)$$

where:

- $\Omega^k = (x|0 \le x_i \le 1; i = 1,\ldots k)$ is an input space factor.
- $1 \le i_1 \ldots < i_s \le k$ and $s = 1,\ldots k$.
- f_0 denotes the mean value of $f(x)$ over the entire domain Ω^k.
- $D_{i_1\ldots,i_s}$ is the partial variance of the model output due to uncertainties in the individual or interaction effects.
- D is the total variance of the output function $f(x)$.

As a result, the first-order sensitivity and the total-effect sensitivity measures are defined as follows:

$$S_i = \frac{D_i}{D} \qquad \text{and} \qquad ST_i = \frac{D_i + \sum_{i\neq j}^{k} D_{ij} + \cdots + D_{12\ldots k}}{D} \qquad (6)$$

Clearly, $0 \le S_i \le ST_i \le 1$, where $\sum_{i=1}^{k} S_i = 1$ and $\sum_{i=1}^{n} ST_i > 1$. If $S_i = ST_i$, this implies that x_i is not involved in any interactions with other input parameters. If $S_i = ST_i = 0$, this means that x_i is not affecting the variance of the model output and, thus, can be fixed. If $S_i = ST_i = 1$, this means that x_i is the only input parameter, which affects the output variance [16].

Thus, this method is based on the estimation of the Sobol's indices that quantify the fractional contribution to the output variance of uncertainties in the inputs:

$$S_{i_1\ldots,i_s} = \frac{D_{i_1\ldots,i_s}}{D} \qquad (7)$$

4.1.1 Monte Carlo Algorithm Method for Sobol's Indices Estimation

The calculation of Sobol indices can be computationally expensive and mathematically demanding [16]. In this work, there are two challenges arising in the calculation of Sobol's indices:

1. The computational cost.
2. The application to the BBN model.

The direct estimation of the S_i and ST_i is computationally expensive: the brute force approach requires N^2 model runs for calculating D_i, D_{ij}, $D_{12\dots k}$, where N is the sample size of input parameters. The Monte Carlo approach reduces the computational cost to $N \times (2 + d)$ model runs, where d is the number of model's inputs [16].

The second challenge refers to the BBN nature of the model developed for premature screen-out risk assessment. The BBN is a stochastic model, which means that the model's output is uncertain. In contrast, the Analysis of Variance (ANOVA) decomposition is derived for deterministic functions. Several authors suggest to use the auxiliary method to solve this computation barrier. However, this method is limited only for the first-order sensitivity measures. Thus, this work proposes a novel method for the estimation of the Sobol's first-order and total-effect indices for BBN models, implemented in the BN Toolbox© in Matlab® [27].

The complete procedure of the Monte Carlo algorithm method for Sobol's indices estimation for the BBN is described in Appendix B.

4.2 Robustness of the BBN Model

Robustness of the BBN model is here interpreted as the insensitivity of its outcomes to small changes in the values of its input parameters. In the specific context of BBN, the attention should be on a distributional robustness given the probabilistic nature of its outcome [24].

In this work, we examine the distribution of the output node "Premature Screen-Out" for different sampling distributions of the input nodes.

Three probability distributions have been considered for the input parameters sampling [22] (see Appendix C):

1. The Gaussian Truncated distribution.
2. The Log-odds distribution.
3. The Uniform Distribution.

The Gaussian Truncated distribution has been utilized to avoid sampling negative values and values larger than 1 for the probabilities of the BBN model. However, the truncation effect leads to an asymmetric distribution, especially for probabilities positioned close to the values of 0 or 1 (refer to Figure 7). The log-odds distribution adds noise to the log-odds form and, thus, has also been considered as sampling distribution. The uniform distribution has been considered for its flexibility and simplicity.

The Gaussian Truncated and Log-odds distributions have been developed using Matlab©.

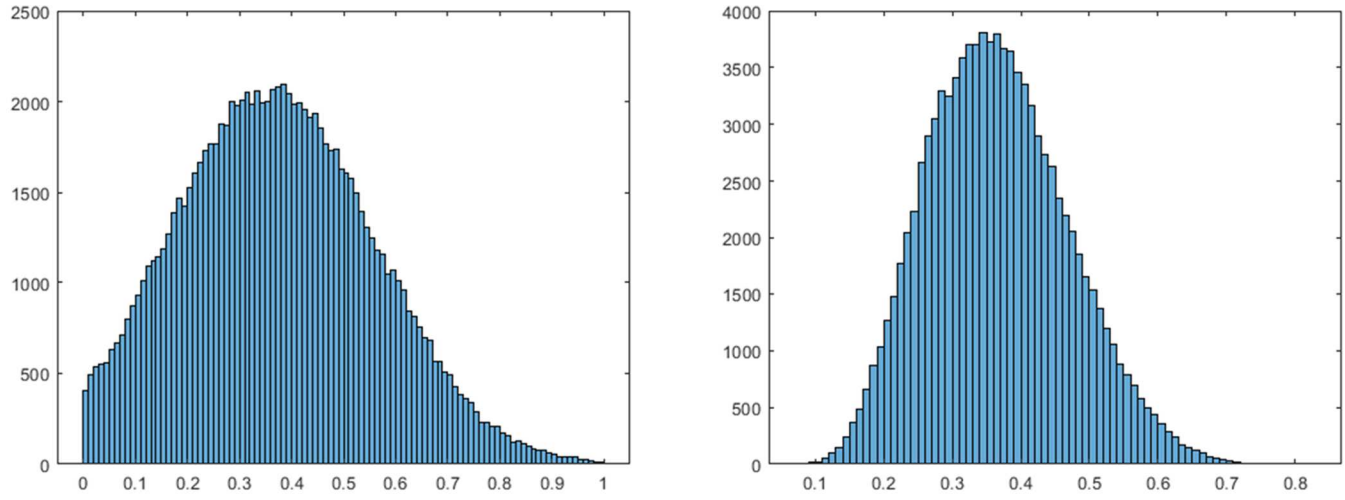

Figure 7 Sampling Distribution for the probability of the node "Natural Fractures", μ_p=0.36 (on the left – Gaussian Truncated distribution, on the right – Log-odds distribution)

5. Risk control

Risk control is the proactive part of the Risk Management and Control process, in which strategies for neutralizing or reducing the identified risks are implemented. The strategies are decided on the basis of the outcomes of the qualitative and quantitative risk assessments, and convert those findings to the evaluation of risk reduction strategies for implementation of the most beneficial ones [1].

5.1 Risk Importance Measures Analysis

For system risk control, it is important to know the impact of the failure of the components on the performance of the system, so as to be able to identify those components whose failure should be prioritarily prevented. For example, the components can be categorized on the basis of Risk Importance Measures (RIM), which quantify the components

failure/unavailability contribution to the overall system failure. However, traditional approaches focus on individual components, with little consideration given to their dependence relations [9].

In the context of BN, these limitations are addressed by extending conventional RIM to scenarios defined as combinations of node states. Bayesian inference can, then, be used to update the systemic risk value on conditions of occurrence or exclusion of a given scenario. This allows scenarios to be ranked in accordance to their impact on the baseline risk by applying RIM.

The RIM can be defined in terms of the utilities associated with the consequences of different system states. The consequences are evaluated at the value node, which, in this work, represents early screen-out, by extracting the probability with which the screen-out occurs. Thus, the disutility function for scenarios is defined as follows [9]:

$$\mathcal{U}[X_u(s_{I(u)})] = \begin{cases} 1, & X_u(s_{I(u)}) \in \mathbb{C}^{fail} \\ 0, & otherwise \end{cases} \quad (8)$$

where

- $X_u(s_{I(u)})$ is the function of the consequences for all combinations of parent states of the value node u.
- $\mathbb{C}^{fail}$ corresponds to the scenarios in which a system fails, i.e. a premature screen-out occurs.

Following Eq. 8, the expected disutility for scenarios S is, then, expressed as the baseline risk:

$$\mathbb{E}[\mathcal{U}] = \sum_{s \in S^+} p(s)\mathcal{U}\left[X_u(s_{I(u)})\right] \quad (9)$$

where the summation is taken over all paths with a strictly positive probability.

In this way, the risk level of scenarios can be assessed by employing the RIM, whose values express the changes in the expected disutility function due to elimination or appearance of a given scenario.

There are different RIM that can be utilized for the scenarios' assessment, such as Risk Share (RS), Risk Achievement Worth (RAW), Risk Reduction Worth (RRW), Birnbaum Importance Measure (BI), and Criticality Importance Measure (CI) [9]. These measures can be used for different Risk Control purposes, such as risk reduction, risk avoidance, risk sharing, etc. The scope of this work is to identify those Risk Control actions that reduce the potential risk exposure, since it examines the impact of the events and properties of the treatment that are monitored and/or considered during the job execution and, thus, cannot be avoided in the design decision making.

For this reason, in this work, the riskiest scenarios are identified by estimating scenarios with large RS. This measure represents the share that can be attributed to the baseline risk. It has the advantage of exactly quantifying the risk reduction, because it can be expressed in terms of the scenario probability [9]:

$$RS\,(\mathbb{S}) = \frac{\mathbb{E}[\mathcal{U}|\,\mathbb{S}]\,p(\mathbb{S})}{\mathbb{E}[\mathcal{U}]} \quad (10)$$

where:

- $p(\mathbb{S})$ is the probability of scenario $\mathbb{S}$.
- $\mathbb{E}[\mathcal{U}|\,\mathbb{S}]$ is the conditional expected disutility function for scenario $\mathbb{S}$.

Other measures, such as RRW and RAW, can also be employed for the evaluation of risk reduction strategies and, thus, have also been considered in this work [9]:

1. The RAW expresses by how much the expected disutility function changes relative to the baseline level, if the scenario occurs. Risk reduction can be implemented by excluding the scenarios with large RAW in order to reduce the baseline risk through relevant corrective actions. If RAW is greater than 1, then the scenario is risky:

$$RAW\,(\mathbb{S}) = \frac{\mathbb{E}[\mathcal{U}|\,\mathbb{S}]}{\mathbb{E}[\mathcal{U}]} \quad (11)$$

2. The RRW gives the relative change in the expected disutility as a result of excluding the scenario. So, if the RRW is greater than 1, then the exclusion of the scenario reduces risk:

$$RRW\,(\mathbb{S}) = \frac{\mathbb{E}[\mathcal{U}]}{\mathbb{E}[\mathcal{U}|\overline{\mathbb{S}}]} \quad (12)$$

where $\mathbb{E}[\mathcal{U}|\overline{\mathbb{S}}]$ is the conditional expected disutility function given the exclusion of scenario $\mathbb{S}$.

If $\mathbb{S} \in \mathbb{S}^{+}$ is the set of scenarios with strictly positive scenario probability, such that p(𝕊) < 1, then the RAW and RRW measures can be expressed in terms of the Risk Share and scenario probability:

$$RAW\,(\mathbb{S}) = \frac{\mathrm{RS}(\mathbb{S})}{p(\mathbb{S})} \quad (13)$$

$$RRW\,(\mathbb{S}) = \frac{1 - p(\mathbb{S})}{1 - \mathrm{RS}(\mathbb{S})} \quad (14)$$

Table 3

Relationships between RIM and scenario probability

x	$RS(\mathbb{S})$	$RAW(\mathbb{S})$	$RRW(\mathbb{S})$
$RS(\mathbb{S})$	x	$\frac{x}{p}$	$\frac{1-p}{1-x}$
$RAW(\mathbb{S})$	px	x	$\frac{1-p}{1-xp}$
$RRW(\mathbb{S})$	$\frac{x-(1-p)}{x}$	$\frac{x-(1-p)}{px}$	x

$p = p(\mathbb{S})$

$x = RS(\mathbb{S})$

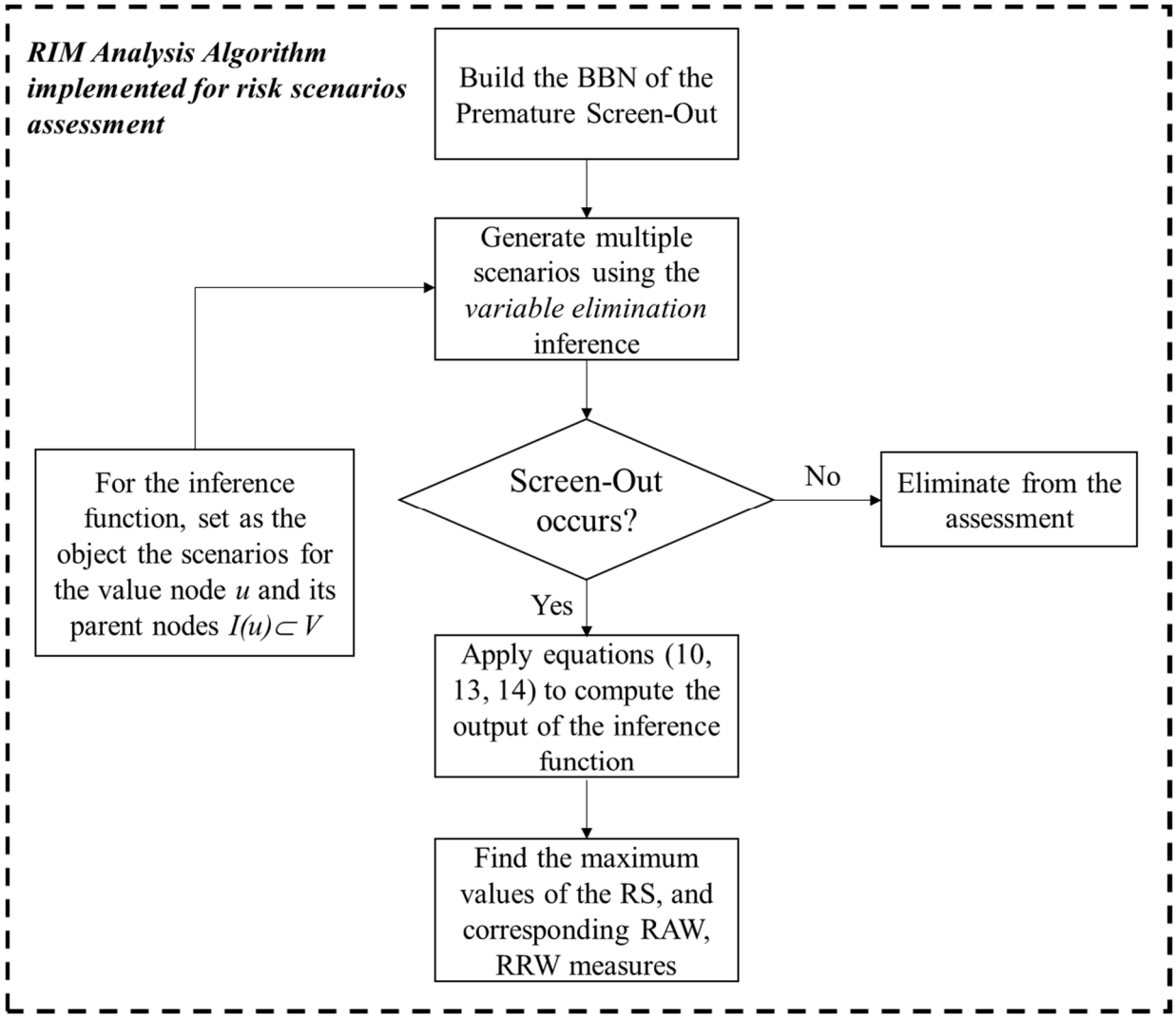

Figure 8 Flowchart of the RIM Analysis Algorithm to evaluate the riskiest scenarios of the BBN

5.2 Cost-Benefit Analysis

In order to reduce the baseline risk, the corrective actions for risk control can be aimed at excluding the "failure" states of those scenarios, which have the greatest impact on the risk of the value node. The selection of best risk mitigation plans can be performed by comparing the values or effects of different actions against the relative cost of a decision, provided that the costs of implementing corrective actions and the cost overruns are known [9]. To this aim, a cost-benefit analysis has been conducted on the possible risk mitigation plans, comparing benefits and costs, here expressed in terms of monetary values.

Table 4 illustrates the general cost overruns due to the occurrence of an early screen-out without considering any corrective action (internal, non disclosable communication Kwantis). When a screen-out occurs, typically the downhole

energy required to clean the wellbore is not enough during proppant flowback. Thus, it is necessary to rig up the coiled tubing, clean out the wellbore and rig down the coiled tubing [6].

Table 4

Common over-expenditure due to a premature screen-out (internal, non disclosable communication Kwantis)

Day	Description	Rig Daily Rate	CT Daily Rate	Frac Package	Material Lost	Perforation
1	Rig Up	100 000$	18 000 $	15 000$	180 000 $	
2	Coiled Tubing Clean-out	100 000$	18 000 $	15 000$		
3	Coiled Tubing Clean-out	100 000$	18 000 $	15 000$		
4	New Perforation Set	100 000$	18 000 $	15 000$		36 000$
						Total
						$748 000,00

Table 5 reports the sample costs associated with each risk mitigation action for the corresponding root cause of an early screen-out (internal, non disclosable communication Kwantis). For example, tortuosity and multiple fractures are mitigated by pumping proppant slugs, i.e. low concentration proppant slurries, in order to erode the near-wellbore fracture restriction and "plug-off" multiple fractures. A 100-mesh sand, i.e. a solid additive, can be used to control an excessive fluid leak-off; it can bridge-off a fracture to limit the fluid invasion into the formation and keep the sand slurry sufficiently hydrated. Low fluid efficiency can be overcome by increasing the pad volume in order to exceed the leak-off rate during the treatment, whereas the reduced fracture width can be increased by setting higher injection rates [6].

Table 5

Risk mitigation strategies (internal, non disclosable communication Kwantis)

Risk	Mitigation	Cost
High Degree of Tortuosity	Pump 2000 lb proppant slugs	2 000$
Multiple Fractures	Pump 2000 lb proppant slugs	2 000$
Low Fluid Efficiency	Increase Pad	40 000$
Excessive Leak-Off	Pump 2000 lb 100-mesh sand	2 000$
Reduced Fracture Geometry	Increase Rate	60 000$
High Max Treating Pressure	New Perforation	36 000$

For each of the riskiest scenarios identified in the RIM Analysis, the different strategies of the mitigation plan must be defined in relation to the failure states of the Premature Screen-Out parent node.

6. Case Study

The developed framework has been applied to a case study of vertical wells. The premature screen-out issue has been assessed qualitatively by identifying the FEP contributing to the screen-out failure (refer to Table 1). The BBN model for the premature screen-out that describes the conditional dependencies between the components of the FEP is illustrated in Figure 6.

6.1 CPT

The quantitative part of the BBN requires the assignment of the probabilities. In this work, the weighted sum algorithm, the log-likelihood method and the elicitation method have been applied. The methods are described in Section 3.

The results of the log-likelihood method have produced the most realistic outcomes although requiring some additional time to calibrate the weights to obtain the target probabilities, as compared to WSA and EBBN methods. As it is shown in Table 6, the parent nodes of the child node "Premature Screen-Out", such as Reduced Fracture Geometry, Degree of Tortuosity and Excessive Leak-Off, are all in their high-order states in all the combinations listed. The probability of the node "Premature Screen-Out" conditioned on these parental combinations generated by WSA and EBBN methods is low (around 0.4), which means that early screen-out is not so likely to occur. However, having high degree of tortuosity, reduced fracture geometry and excessive leak-off not mitigated is sufficient to lead to the premature screen-out and this is consistent with the outcomes of the log-likelihood method.

In the EBBN method, the more parent nodes considered for a child, the less the value of the weight obtained since the denominator of the formula for w_i in Eq.19 is equal to the sum of probabilities of all parent nodes. This leads to small values of the probabilities of the child node for medium- and big-size matrices, which should instead be high, as more failure (high-order) states of parent nodes are considered.

In the WSA method, the influence weights of the parent nodes on the child node are normalized so that $0 \leq w_i \leq 1$ and $\sum_{i=1}^{N} w_i = 1$. Also in this case, the more parent nodes, the smaller the values of the relative weights obtained minimising $w_i P\left(x_c^m \middle| \left\{Comp\left(X_{pi} = x_{pi}^{ji}\right)\right\}\right)$ and, correspondingly, the smaller the target probability of the conditioned child node.

Table 6

CPT Results

Parental combination							P(Premature Screen-Out – Yes)		
Reduced Fracture Geometry	Degree of Tortuosity	Excessive Leak-Off	Fluid Efficiency	Poor Erosion	Multiple Fractures	Max Treating Pressure	WSA	EBBN	Log-likelihood
Yes	High	Yes	Low	No	No	Low	0.35	0.26	0.97
Yes	High	Yes	Low	No	No	High	0.39	0.33	0.99
Yes	High	Yes	Low	No	Yes	Low	0.45	0.36	1

Based on the above considerations, the log-likelihood results have been used as input for the inference computations in the BBN.

6.2 Sensitivity Analysis Results

In this section, we examine the sensitivity of the BBN model to its input probabilities by using the Sobol's variance decomposition method described in Section 4.1.

In total, the expert analysts have chosen 24 input probability parameters (refer to Table E-1) for the investigation of their influence on the model output of probability of premature screen-out.

The sensitivity results (refer to Table 7) show that the probabilities of the nodes with no parents are more influential to the model output. In addition, the larger the number of child nodes affected by a parent node, the more that parent node affects the output. For example, in the BBN model for Premature Screen-Out in Figure 6, the node "Degree of Tortuosity" is the node that has the highest number of causal arcs and, correspondingly, in the sensitivity analysis shows that the conditional probabilities of this node are among the most influential parameters (Sobol's index first order - 0.09, total order – 0.11). This node is conditioned on the parent nodes, "Perforation Friction" and "NWB Friction", which are the most influential nodes without parents (Sobol's index first order - 0.29, total order – 0.33). This can be explained by the frequency of the appearance of these probabilities in the Cartesian Product computation since they have to be considered in each joint probability distribution of the node "Degree of Tortuosity" and other nodes followed by the causal arcs.

The sensitivity results support the fact that tortuosity is one of the main root causes of premature screen-out, and that variables such as NWB Friction and Perforation Friction are important be monitored prior to the MiniFrac jobs, in order to guarantee good communication between the wellbore and the main fracture (refer to Table 7) [6].

Another influential variable, which is also believed to be one of the major causes of early screen-outs, is the Natural Fissures. These fissures may obstacle the fracture behavior, leading to excessive leak-off and reduced fracture geometry (refer to Table 7) [6].

These results correctly represent the expectations of expert experience and literature overview and, consequently, validate the integrity of the model's structure.

As for the type of sampling distribution, this seems not to affect the outcome of the analysis: the calculations carried out sampling from different distributions have led approximately to the same results (refer to Appendix F).

Table 7

Results of the Sobol's sensitivity analysis

Input parameters	First-order	Total Order
P(NWB Friction)	0.29	0.33
P(Perforation Friction)	0.29	0.33
P(Degree of Tortuosity | NWB Friction)	0.09	0.11
P(Degree of Tortuosity | Perforation Friction)	0.09	0.11
P(Natural Fractures)	0.09	0.11

6.3 Uncertainty Analysis Results

In this section, we examine the robustness of the BBN model to its input probabilities (refer to Table E-1), with the uncertainty analysis described in Section 4.2.

Table 8 represents the values of the mean, variance, minimum, maximum and range of variation of the marginal probability distribution of the Premature Screen-Out output, resulting from different sampling distributions of the input probability values. The histograms of the output distribution are shown in Figure 9 and Figure 10. The results show that the BBN model is robust to small variations in its input probabilities and demonstrates the realistic behavior. The distribution of the output node "Premature Screen-Out" corresponding to the different input probability sampling distributions (refer to Section 4.2) follows approximately a Gaussian distribution and the mean value of the distribution is stable around 0.79 (refer to Figure 9, Figure 10 and Table 8). The variability of the output distribution also shows a small variation as expected getting smaller with smaller standard deviations of the input probability sampling distributions (refer to Table 8).

Table 8

Results of the uncertainty analysis of the distribution of the output node "Premature Screen-Out"

Distribution	Sampling Design	Mean of the output	Variance of the output	Minimum of the output distribution	Maximum of the output distribution	Range
Gaussian Truncated Distribution	$\sigma_1 = 0.1$	0.7924	0.0019	0.6202	0.9002	0.2800
	$\sigma_2 = 0.15$	0.7966	0.0042	0.5323	0.9449	0.4126
	$\sigma_3 = 0.2$	0.8006	0.0066	0.4655	0.9673	0.5018
Log-odds Distribution	$\sigma_1 = 0.1$	0.7906	5.369e-04	0.7111	0.8519	0.1408
	$\sigma_2 = 0.15$	0.7911	0.0011	0.6678	0.8784	0.2106
	$\sigma_3 = 0.2$	0.7917	0.0020	0.6238	0.9013	0.2775
Uniform Distribution	$a = \mu_p - 0.1$ $b = \mu_p + 0.1$	0.7897	6.737e-04	0.6928	0.8605	0.1677

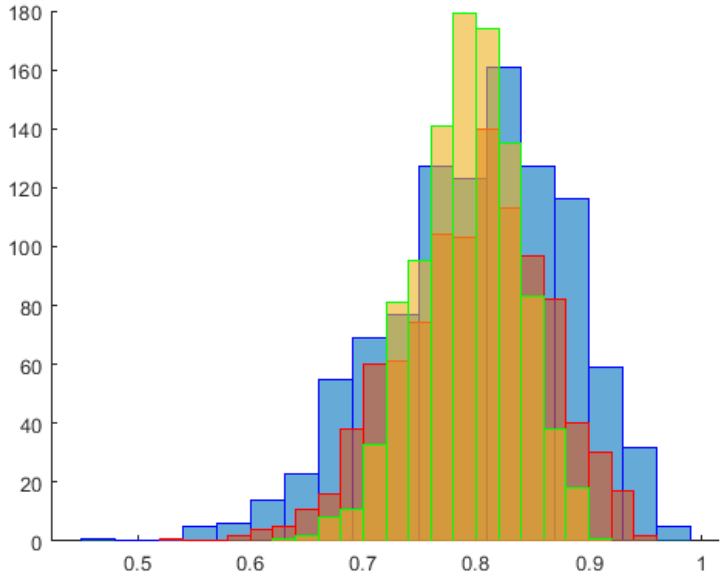

Figure 9 Output Distribution for the Gaussian Truncated Sampling (green edges correspond to $\boldsymbol{\sigma_1 = 0.1}$, red to $\boldsymbol{\sigma_2 = 0.15}$, and blue to $\boldsymbol{\sigma_3 = 0.2}$)

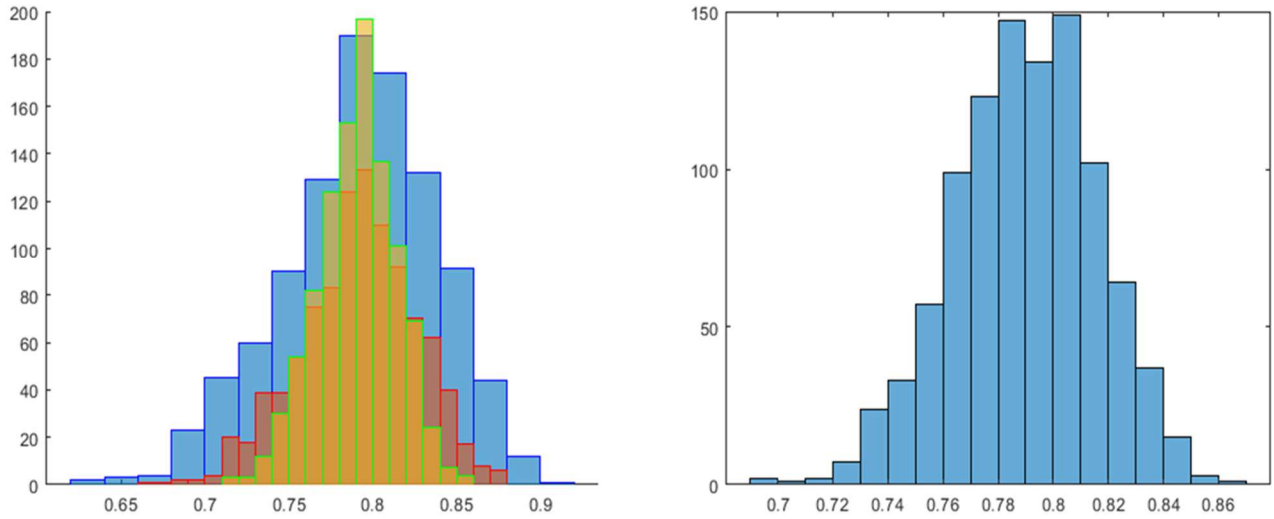

Figure 10 Output Distribution for the Log-odds (left) and Uniform (right) Sampling. In the Log-odds sampling, green edges correspond to $\boldsymbol{\sigma_1 = 0.1}$, red to $\boldsymbol{\sigma_2 = 0.15}$, and blue to $\boldsymbol{\sigma_3 = 0.2}$.

6.4 Uncertainty Reduction

The probabilities (refer to Table E-1) of the most influential input parameters (refer to Table 7) have been re-assessed differently to explore the effect of uncertainty reduction on the probability of Premature Screen-Out. The mean values are given in Table 9 and have been obtained based on the following considerations:

1. The only available data for the probability evaluation relate to the NWB Friction and Perforation Friction parameters. The data set for the friction losses contains continuous data and the probabilities of NWB Friction and Perforation Friction have been defined using the goodness of fit test for individual distribution identification, based on the Anderson-Darling (AD) test and the P-values. To prove the results of the goodness of fit test, the histogram with fit of different distributions has been constructed. The graphs in Figure 11 provide good examples of the distribution fitting of the sample data.

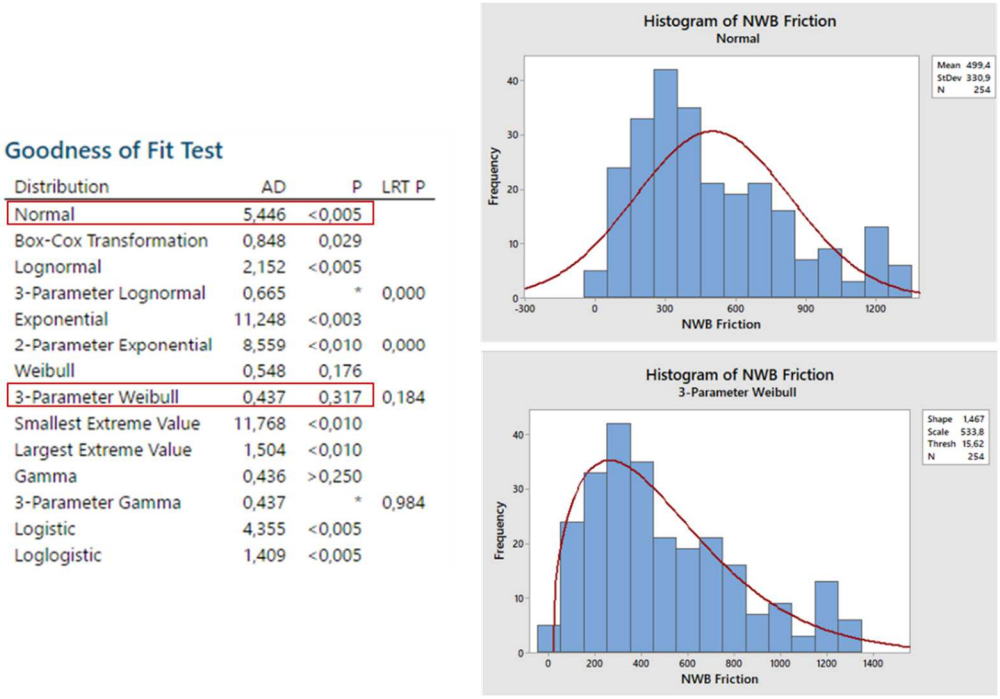

Figure 11 Probability Distribution Fitting Analysis

2. The probability of occurrence of the Natural Fractures event has been estimated by the frequentist approach using the historical observations from the database.

3. There are missing data about the relationship between the occurrence of tortuosity and friction losses values (refer to Section 3). Therefore, these probabilities have been re-evaluated directly by company experts using a probability scale. Although the subjectivity of additional expert judgement may include some uncertainty, in this case the re-evaluation considered the high/low level of the state for the NWB and Perforation frictions in terms of psi that gives the high probability of having tortuosity.

As a result, the probability of premature screen-out changes from 0.78 to 0.67 (refer to Table 9). The smaller value of probability of screen-out obtained with the re-evaluation is consistent with the case study of vertical wells. This can be explained by the fracture initiation process, as opposed to the deviated wells, where the risks of having the premature screen-out are higher due to additional effects of more complicated fracture geometries obtained during a fracturing job [6].

Table 9

Results of the probabilities re-evaluation

Input Parameters	Probabilities		
	Before Sensitivity Analysis	After Sensitivity Analysis	Difference percentage
P(High NWB Friction)	0.6	0.18	**-70%**
P(High Perforation Friction)	0.6	0.36	**-40%**
P(Degree of Tortuosity |High NWB Friction)	0.5	0.9	**+80%**
P(Degree of Tortuosity |High Perforation Friction)	0.5	0.9	**+80%**
P(Natural Fractures)	0.36	0.25	**-31%**
P(Premature Screen-Out)	0.78	0.67	**-14%**

6.5 Risk Importance Measures Results

In this section, we evaluate the riskiest scenarios for Premature Screen-Out by applying the RIM analysis illustrated in Section 5.1.

Table 10 demonstrates the five riskiest scenarios for Premature Screen-Out given the states of its parent nodes, with its conditional probabilities for each scenario, the joint probabilities and the RIM of each scenario.

Figure 12 shows the probabilities of the "failure" (high-order) states of the BBN model nodes, given the evidence that the Premature Screen-Out has occurred. As seen earlier, events such as Degree of Tortuosity, Multiple Fractures and Reduced Fracture Geometry, have a significant impact on the value of the output node of Premature Screen-Out and should be considered with high priority in the risk reduction plan (refer to Figure 12). These results are consistent with the results of the RIM analysis, in which these events appear in all five riskiest scenarios (except for the node "Degree of Tortuosity in the third scenario – refer to Table 10).

Table 10

Five riskiest scenarios from RIM Analysis

Scenario	Degree of Tortuosity	Poor Erosion	Max Treating Pressure	Multiple Fractures	Excessive Leak-Off	Fluid Efficiency	Reduced Fracture Geometry	$p(s_{screenout} \mid S_I)$	$p(\mathbb{S})$	RS	RAW	RRW
1	High	No	Yes	Yes	No	High	Yes	1	0.136	0.204	1.49	1.084
2	High	No	No	Yes	No	High	Yes	0.99	0.067	0.1	1.49	1.037
3	Low	No	No	Yes	No	High	Yes	0.873	0.049	0.074	1.49	1.026
4	High	No	Yes	Yes	Yes	Low	Yes	1	0.047	0.07	1.49	1.025
5	High	No	Yes	Yes	Yes	High	Yes	1	0.043	0.065	1.49	1.023

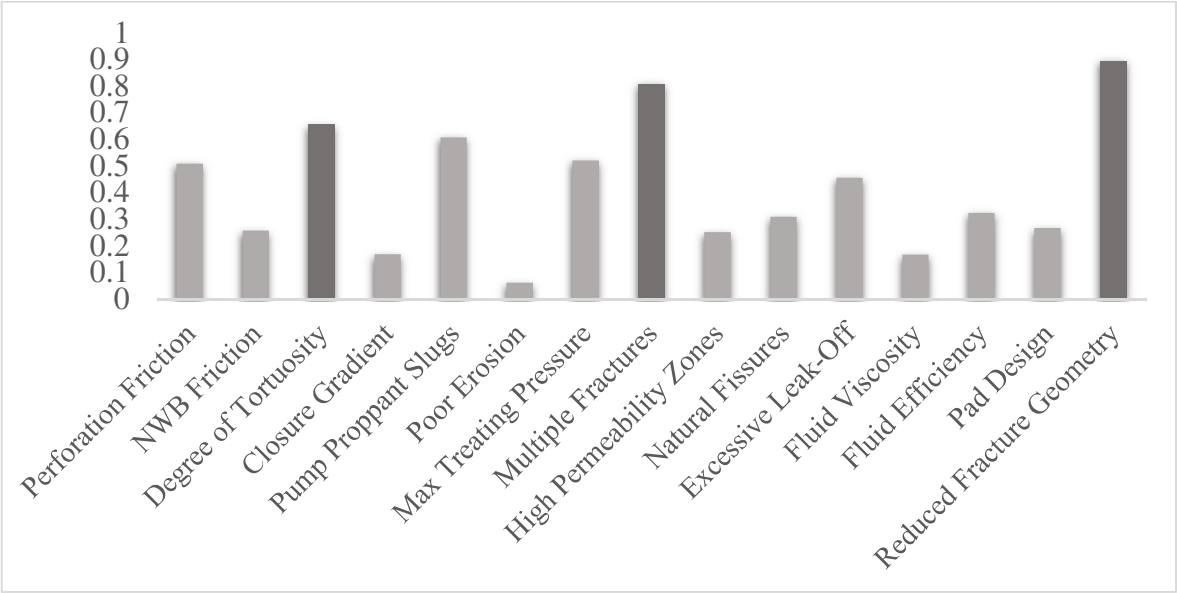

Figure 12 Bar chart of the probabilities of the "failure" states of the BBN model nodes for P (Premature Screen-Out) = 1

6.6 Cost-Benefit Analysis Results

In this section, we evaluate different mitigation plans in accordance with the five riskiest scenarios listed in Table 10.

Table 11 shows the mitigation plans and associated strategies, the costs of carrying out the operations, the probability of early screen-out after the mitigation and the difference with the probability of the screen-out, before and after the mitigation plan.

Table 11

Mitigation plans with associated costs and the reduction of the probability of Premature Screen-Out

Mitigation plan	Risks mitigated	Mitigation costs (example)	Probability of Premature Screen-Out after mitigation	Difference percentage
1	High Degree of Tortuosity, Multiple Fractures, Reduced Fracture Geometry, Max Treating Pressure	$100 000	9,78%	-85%
2	High Degree of Tortuosity, Multiple Fractures, Reduced Fracture Geometry	$64 000	12,41%	-81%
3	Multiple Fractures, Reduced Fracture Geometry	$62 000	16,01%	-76%
4	High Degree of Tortuosity, Multiple Fractures, Reduced Fracture Geometry, Low Fluid Efficiency, Excessive Leak-Off, Max Treating Pressure	$142 000	0,11%	-100%
5	High Degree of Tortuosity, Multiple Fractures, Reduced Fracture Geometry, Excessive Leak-Off, Max Treating Pressure	$102 000	0,52%	-99%

Table 12 illustrates the cost-benefit analysis, where:

1. Weighted Impact before and after mitigation is the result of multiplication of the screen-out probability by its impact in terms of over expenditure before and after mitigation, accordingly.

2. Benefit, i.e. assumed savings, is calculated as the difference between the weighted impacts costs before/after mitigation and the mitigation costs.

As per the carried out analysis, corrective action plan 5 is the best approach, since it achieves significant reduction of the baseline risk without imposing too high costs (refer to Figure 13).

Table 12

Cost-Benefit Analysis of the Mitigation Plans

Probability of Premature Screen-Out before mitigation	Impact: Opex increase	Weighted impact before mitigation	Mitigation plan	Mitigation costs	Probability of Premature Screen-Out after mitigation	Weighted impact after mitigation	Benefit
			1	$100 000	9,78%	$73 154,40	$328 005,60
			2	$64 000	12,41%	$92 826,80	$344 333,20
67%	$748 000,00	$501 160,00	3	$62 000	16,01%	$119 754,80	$319 405,20
			4	$142 000	0,11%	$822,80	$358 337,20
			5	***$102 000***	***0,52%***	***$3 889,60***	***$395 270,40***

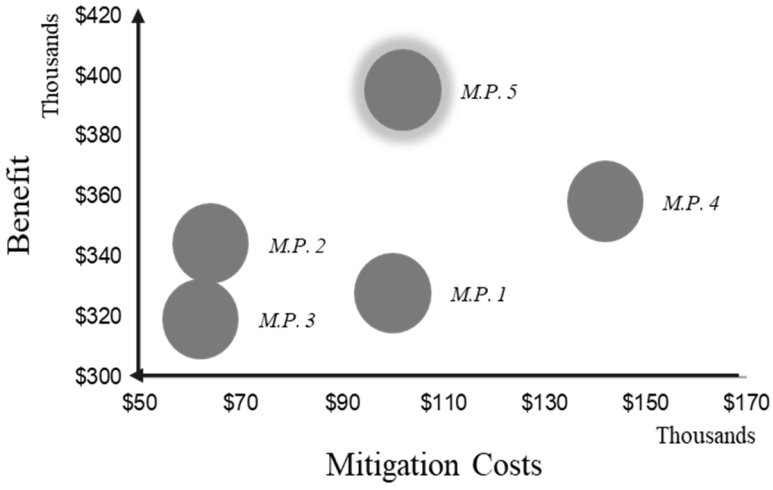

Figure 13 Cost-Benefit Analysis (M.P. – Mitigation Plan)

7. Conclusions

Premature screen-outs are causes of failure of the hydraulic fracturing jobs and lead to loss of working days and cost overruns. Numerous factors, related to physical properties of the geological formation, reservoir properties and characteristics of the treatment design, may lead to such problems. The diagnostic methods currently applied only give signals of early screen-out and try to identify the potential causes during job execution. On the contrary, it is important to predict the probability of occurrence of screen-outs and identify in advance the riskiest scenarios, in order to define a priori risk reduction actions that can effectively avoid screen-out.

In this work, the premature screen-out issue has been addressed through a complete framework for implementation within a practical Risk Management and Control Process. The qualitative identification of the hazards contributing to the premature screen-out has been defined through FEP identification. The quantitative assessment is based on the modelling framework offered by Bayesian Belief Networks. The input probabilities of the BBN model have been assessed by expert elicitation methods due to shortfall in data, and the log-likelihood method has turned out to provide the best results. The model's robustness and its sensitivity to input parameters have been assessed by performing uncertainty analysis and sensitivity analysis by the Sobol's variance decomposition method. The results of the uncertainty analysis have shown that the model is robust. Furthermore, the results of the sensitivity analysis endorse the knowledge that the tortuosity is a major cause of screen-outs and, therefore, it should be treated carefully during the hydraulic fracturing operation. The probabilities of the most influential variables as identified by the sensitivity analysis have been re-evaluated using historical observations and additional experts judgements for the case study of vertical wells in a specified region. As a result, the probability of screen-out has decreased. The riskiest scenarios of premature screen-out have been identified by risk importance measures analysis and the best risk reduction plans have been determined by cost-benefit analysis. The statistics of screen-outs in vertical wells accounts for 10% of all operations done, which is consistent with the risk results after cost-benefit analysis.

In summary, the proposed framework offers a novel approach for predicting the risk of premature screen-outs based on the BBN model, identification of the most influential variables by sensitivity analysis, and the choice of risk mitigation strategies guided by the outcomes of risk importance measures analysis and cost-benefit analysis.

Acknowledged: The authors wish to thank Dr. Xuefei Lu for her guidance in the uncertainty and sensitivity analyses, and for her assistance to the editing of the paper.

8. Appendix A

Weighted Sum Algorithm. The CPT in the WSA method is constructed as follows:

$$P\left(x_c^m | x_{p_1}^{j_1}, x_{p_2}^{j_2}, \dots, x_{p_N}^{j_N}\right) = \sum_{i=1}^{N} w_i P\left(x_c^m | \left\{Comp\left(X_{p_i} = x_{p_i}^{j_i}\right)\right\}\right) \qquad (15)$$

where:

- w_i is the relative influence weight of the *ith* parent node on the X_c child node.
- x_c^m is the *mth* state of the child node X_c.
- $x_{p_2}^{j_2}$ is the second state of the second parent node X_{p_2}.
- $x_{p_N}^{j_N}$ is the *Nth* state of the *Nth* parent node X_{p_N}.
- $Comp\left(X_{p_i} = x_{p_i}^{j_i}\right)$ is a compatible parental configuration for the *ith* state *j* of the *ith* parent node.

In this method, the elicitation consists of defining the following two sets of parameters [15]:

1. The relative weights $w_1, \dots, w_N$ of the parent nodes of a child node, where $0 \leq w_i \leq 1$ and $\sum_{i=1}^{N} w_i = 1$. The relative influence weight shows the relation of a parent-child node pair, i.e. the degree of influence of a parent node on its child node. The calculation of the influence weight initiates from assigning a non-normalized relative weight of parent nodes on their child in terms of degree of influence (for example, low-medium-high). Then, each degree of influence is given a value – for example, 2 for "low" influence, 4 for "medium", 6 for "high" (refer to Table A-1). The influence weights are, then, defined by normalizing the assigned values, so that the sum of all weights of the parent nodes is equal to 1. For example, if the weight for a parent-child pair is equal to 0, this indicates that the child node is not affected by the parent node (there is no link in the BBN) and, therefore, the parent node can be excluded from the Table; conversely, if the weight is equal to 1, this indicates that the corresponding parent node is the only determinant of its child node.
2. The probability distributions for compatible parental configurations.

Log-likelihood method. The elicitation procedure in the Log-likelihood method consists of the following steps [15]:

1. Identify a typical distribution of a child node, T_r.
2. Set the base of the log form, *b*.
3. Determine the weighting factor, β_{x_c}, for each state of the child node x_c.
4. Assess the weighting factor, $\alpha_{x_{pi}}$, for each state of the parent nodes on the child node, in a scale from very low to very high and convert into a numerical scale.

As a result, we get the influence weight parameter of the *ith* parent node on a child node X_c.:

$$\gamma_{x_c x_{pi}} = \beta_{x_c} \alpha_{x_{pi}} \qquad (16)$$

and the $log_b L$ – log likelihood of the state of child node x_c, given the states for each of the parent nodes, x_{pi}:

$$log_b L(x_c | x_{p1}, x_{p2}, \dots x_{pN}) = \sum_{i=1}^{N} \gamma_{x_c x_{pi}} \qquad (17)$$

In this method, the principle of assigning the influence weight is similar to the WSA method. However, the assignment of influence is associated with the states of the nodes and the weighting factors of the states are given positive or negative signs. The choice of the sign of the weighting factor for the parent state should be based on the assumption of the probability of the state of a child node – it should be of the same sign as the child state's weight if it results in a high probability of a child state and opposite to the child state's weight if it results in a small probability of a child state.

The assignment of weights for each pair of states of parent and child nodes makes the algorithm more flexible than other methods, because it considers both the positive and negative influences. For example, if the parameter $\gamma_{x_c x_{pi}}$ is positive, the probability for that combination increases and if the parameter is negative – the probability decreases accordingly [15].

Table A-1

Influence assignment for the parent nodes of the node "Degree of Tortuosity"

	Degree of Tortuosity				
	Very Low	Low	Medium	High	Very High
Perforation Friction				x	
NWB Friction				x	

EBBN method. The procedure of CPT generation using the EBBN method is implemented as follows [15]:

5. For every parent node $X_{pi} \in pa(X_c)$, order the states in a way that it has either a negative or a positive influence on the child node, X_c.

6. For every state x_c of child node, X_c, determine the assignment so that the probability $P(X_c = x_c|a_{xc})$ is as large as possible.

7. For every parent node evaluate those probabilities in which $X_{pi} \in pa(X_c)$ is in its most favorable state for "failure" states of X_c and all $X_{pi} \in pa(X_c)$ are in their least favorable state for "failure" states of X_c.

The conditional probabilities for CPT are derived using [15]:

$$P(X_c = x_c^m|pa(X_c) = a) = \sum_{i:X_{pi}|pa(X_c)} w_i * \frac{\int_{I_{min}}^{I_{max}} f_{x_c^m}(I_{joint}(a))dI_{joint}(a)}{\max(I_{ind}(x_{pi}^j), I_{joint}(a)) - \min(I_{ind}(x_{pi}^j), I_{joint}(a))} \quad (18)$$

where a is the assignment of states of parent nodes and w_i is the influence weight for every parent node:

$$w_i = \frac{1}{2}\frac{\delta_i^+}{\sum_{n:X_{pN}\in pa(X_c)}\delta_n^+} + \frac{1}{2}\frac{\delta_i^-}{\sum_{n:X_{pN}\in pa(X_c)}\delta_n^-} \quad (19)$$

where:

$$\delta_i^+ = P\left(X_c = x_c^{max}\middle|a_{neg,p^+}\right) - P(X_c = x_c^{max}|a_{neg}) \quad (20)$$

$$\delta_i^- = P\left(X_c = x_c^{min}\middle|a_{neg}\right) - P\left(X_c = x_c^{min}\middle|a_{neg,p^+}\right) \quad (21)$$

- X_{max} – the highest ordered ("failure") state.

- X_{min} – the lowest ordered ("success") state.

- a_{neg,p^+} – the assignment of a parent node in which one of the parents is in its most favorable state for "failure" states of a child node and all other parent nodes are in their least favorable states.

- a_{neg} – the assignment, in which all the parent nodes are in their most favorable state for "success" states of the child node.

I_{ind} and I_{joint} are the individual and joint influence factors of parent nodes on the child node [15]:

$$I_{ind}\left(x_{pi}^{j}\right) = \begin{cases} \dfrac{rank(x_{pi}^{j}) - 1}{rank(x_{pi}^{max}) - 1}, & if\ S^{+}(X_p, X_c) \\ \dfrac{rank(x_{pi}^{max}) - rank(x_{pi}^{j})}{rank(x_{pi}^{max}) - 1}, & if\ S^{-}(X_p, X_c) \end{cases} \quad (22)$$

$$I_{joint}(a) = \frac{\sum_{\{i:X_{pi}\epsilon pa(X_c)} I_{ind}\left(x_{pi}^{j}\right) * (rank(x_{pi}^{j}) - 1)}{\sum_{\{i:X_{pi}\epsilon pa(X_c)} (rank(x_{pi}^{max}) - 1)} \quad (23)$$

$S^{+}(X_p, X_c)$ represents a positive influence on X_c and $S^{-}\left(X_p, X_c\right)$, on the contrary, represents a negative influence.

Table A-2

Assignment of Probabilities for the EBBN method

Configuration of the parent nodes states		**P(Excessive Leak-Off)**	
Natural Fractures	High Permeability Zones	No	Yes
No	No	0.9	0.1
Yes	Yes	0.01	0.99
Yes	No	0.1	0.9
No	Yes	0.1	0.9

9. Appendix B

In our work, the BBN model's output function $y = f(x)$ is the inference function to compute the marginal probability of having an early screen-out, $p(X_{screenout}) = \sum \prod_{i=1}^{N} p(X_{screenout}|Parents(X_{screenout}))$, whereas the input parameters are expressed in terms of marginal, $p(s_i)$, and conditional probabilities, $p(s_i\ |S_I)$.

The procedure to calculate the Sobol's indices for the BBN using the Monte Carlo method consists of the following steps:

1) Generate a $N \times 2d$ sample matrix for the input parameters, i.e. the marginal and conditional probabilities, in accordance with their probability distributions. Define two matrices *A* and *B,* each taken as half of the $N \times 2d$ sample matrix

$$\mathrm{A} = \begin{bmatrix} p(s_1)^{(1)} & p(s_2)^{(1)} & \dots & p(s_k)^{(1)} \\ p(s_1)^{(2)} & p(s_2)^{(2)} & \dots & p(s_k)^{(2)} \\ \vdots & \vdots & \vdots & \vdots \\ \dots & \dots & \dots & \dots \\ p(s_1)^{(N)} & p(s_2)^{(N)} & \dots & p(s_k)^{(N)} \end{bmatrix} \quad (24)$$

$$\mathrm{B} = \begin{bmatrix} p(s_{k+1})^{(1)} & p(s_{k+2})^{(1)} & \dots & p(s_{2k})^{(1)} \\ p(s_{k+1})^{(2)} & p(s_{k+2})^{(2)} & \dots & p(s_{2k})^{(2)} \\ \vdots & \vdots & \vdots & \vdots \\ \dots & \dots & \dots & \dots \\ p(s_{k+1})^{(N)} & p(s_{k+2})^{(N)} & \dots & p(s_{2k})^{(N)} \end{bmatrix} \quad (25)$$

2) Create a third matrix, C, containing all the sample values of matrix A, but with the *i*-th column taken from matrix B:

$$\mathrm{C} = \begin{bmatrix} p(s_1)^{(1)} & p(s_i)^{(1)} & \dots & p(s_k)^{(1)} \\ p(s_1)^{(2)} & p(s_i)^{(2)} & \dots & p(s_k)^{(2)} \\ \vdots & \vdots & \vdots & \vdots \\ \dots & \dots & \dots & \dots \\ p(s_1)^{(N)} & p(s_i)^{(N)} & \dots & p(s_k)^{(N)} \end{bmatrix} (26)$$

3) Estimate the output distribution of the marginal probability of the early screen-out for each sample from the input probabilities of the matrices A, B and C by using the BN Toolbox ©.

4) Compute the first-order and total-effect sensitivity measures using the estimators below:

$$S_i = \frac{D_i}{D} = \frac{D - \frac{1}{2N}\sum_{j=1}^{N}\left[f(B_j) - f(C_j)\right]^2}{\frac{1}{N}\sum_{j=1}^{N} f^2(A_j) - \left(\frac{1}{N}\sum_{j=1}^{N} f(A_j)\right)^2} \quad (27)$$

$$ST_i = \frac{D_i^{tot}}{D} = \frac{\frac{1}{2N}\sum_{j=1}^{N}\left[f(A_j) - f(C_j)\right]^2}{\frac{1}{N}\sum_{j=1}^{N} f^2(A_j) - \left(\frac{1}{N}\sum_{j=1}^{N} f(A_j)\right)^2} \quad (28)$$

where:

- D_i is a partial variance of the model output due to uncertainties in the individual effects of x_i.

- D_i^{tot} is the partial variance of the model output due to uncertainties in the individual effects of x_i and interaction effects of x_i, x_j, and so on.

- A_j, B_j, C_j are the *jth* row vector of the input values in the matrices of A, B and C respectively.

5) Rank the parameters according to the values of the sensitivity indexes computed.

10. Appendix C

Table C-1 reports the input sampling distribution for both sensitivity and uncertainty analyses.

Table C-1

Sampling distributions for the sensitivity and uncertainty analyses

Type of a Distribution	Probability Density Function	Sampling Design
Gaussian Truncated Distribution	$f(x) = \frac{1}{\sigma_N} \frac{\phi(\frac{x-\mu}{\sigma_N})}{\Phi\left(\frac{b-\mu}{\sigma_N}\right) - \Phi\left(\frac{a-\mu}{\sigma_N}\right)}$	$\mu = p(X_i)$ $a = 0$ $\sigma_1 = 0.1$ $b = 1$ $\sigma_2 = 0.15$ $\sigma_3 = 0.2$
Log-odds Distribution	$f(x) = log\frac{p}{1-p} + \epsilon \quad for\ x \in [0,1],$ $where\ \epsilon \sim N(0, \sigma_N)^*$	$p = p(X_i)$ $\sigma_1 = 0.1$ $\sigma_2 = 0.15$ $\sigma_3 = 0.2$
Uniform Distribution	$f(x) = \frac{1}{b-a} \quad for\ x \in [a, b]$	$a = p(X_i) - 0.1$ $b = p(X_i) + 0.1$

$^*\epsilon$ *is a noise term assumed to follow standard normal distibution*

11. Appendix D

In this work, the suggested number of simulation runs is 10000. Figure D-1 shows the results of the sensitivity analysis performed according to different simulation runs - 1000, 5000 and 10000. As it is shown, the order of the input parameters is the same. However, in cases of 1000 and 5000 simulation runs the Total Order sensitivity indices of some parameters are less than the First-Order sensitivity indices, which contradicts the fact of $\mathbf{0} \leq \boldsymbol{S_i} \leq \boldsymbol{ST_i} \leq \mathbf{1}$.

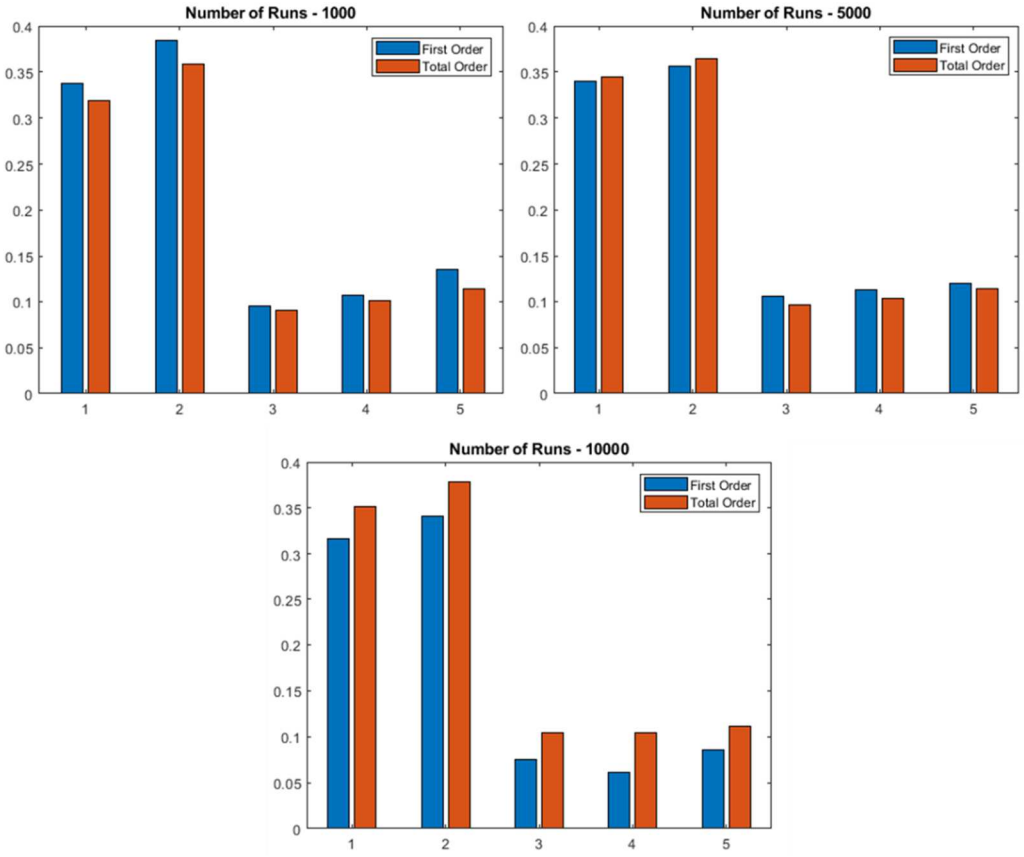

Figure D-1 First-Order and Total Order sensitivity indices according to different simulation runs (on the x-axis: 1 corresponds to the P(Perforation Friction), 2 – P(NWB Friction), 3 – P(Degree of Tortuosity |High Perforation Friction), 4 - P(Degree of Tortuosity |High NWB Friction), 5 - P(Natural Fissures))

12. Appendix E

Table E-1

Input probability parameters sampled for sensitivity and uncertainty analyses

Input Probability Parameters	Probability
P(Perforation Friction)	0.60
P(NWB Friction)	0.60
P(Closure Gradient)	0.15
P(Pad Design)	0.23
P(Natural Fissures)	0.36
P(High Permeability Zones)	0.36
P(Fluid Viscosity)	0.15
P(Pump Proppant Slugs |Degree of Tortuosity)	0.90
P(Poor Erosion)	0.10
P(Degree of Tortuosity |NWB Friction)	0.50
P(Degree of Tortuosity |Perforation Friction)	0.50
P(Max Treat Pressure |Poor Erosion)	0.09
P(Max Treat Pressure |Degree of Tortuosity)	0.61
P(Max Treat Pressure |Closure Gradient)	0.76
P(Fluid Efficiency | Fluid Viscosity)	0.66
P(Fluid Efficiency |Excessive Leak-off)	0.44
P(Excessive Leak-Off |High Permeability Zones)	0.76
P(Excessive Leak-Off |Natural Fissures)	0.89
P(Reduced Fracture Geometry |Degree of Tortuosity)	0.33
P(Reduced Fracture Geometry |Pad Design)	0.89
P(Reduced Fracture Geometry |Natural Fissures)	0.33
P(Reduced Fracture Geometry |Multiple Fractures)	0.55

13. Appendix F

Table F-1

Sobol's sensitivity analysis results for the Uniform Distribution Sampling

Uniform Distribution Ranking			
Parameter	First-order	Parameter	Total order
P(Perforation Friction)	0.3239	P(Perforation Friction)	0.3323
P(NWB Friction)	0.2894	P(NWB Friction)	0.2932
P(Degree of Tortuosity |High Perforation Friction)	0.0938	P(Natural Fissures)	0.1084
P(Degree of Tortuosity |High NWB Friction)	0.0934	P(Degree of Tortuosity |High NWB Friction)	0.1038
P(Natural Fissures)	0.0893	P(Degree of Tortuosity |High Perforation Friction)	0.0988
P(Pad Design)	0.0572	P(Pad Design)	0.0574
P(Closure Gradient)	0.0392	P(High Permeability Zones)	0.0286
P(High Permeability Zones)	0.0235	P(Closure Gradient)	0.0267
P(Fluid Viscosity)	0.0208	P(Fluid Viscosity)	0.0222
P(Fluid Efficiency |Excessive Leak-Off)	0.0173	P(Fluid Efficiency |Excessive Leak-Off)	0.0129
P(Reduced Fracture Geometry |Natural Fissures)	0.0021	P(Reduced Fracture Geometry |Natural Fissures)	0.0098
P(Excessive Leak-Off |Natural Fissures)	0.0018	P(Excessive Leak-Off |Natural Fissures)	0.0066
P(Reduced Fracture Geometry |Multiple Fractures)	0.0015	P(Excessive Leak-Off |High Permeability Zones)	0.0066
P(Fluid Efficiency |Low Fluid Viscosity)	0.0013	P(Reduced Fracture Geometry |Multiple Fractures)	0.0049
P(Excessive Leak-Off |High Permeability Zones)	0.0013	P(Max Treat Pressure |High Closure Gradient)	0.0011
P(Reduced Fracture Geometry |Pad Design)	0.0011	P(Reduced Fracture Geometry |Pad Design)	0.0009
P(Max Treat Pressure |High Closure Gradient)	0.0004	P(Fluid Efficiency |Low Fluid Viscosity)	0.0003
P(Poor Erosion)	0.0002	P(Poor Erosion)	0.0002
P(Pump Proppant Slugs |Degree of Tortuosity)	0.0001	P(Pump Proppant Slugs |Degree of Tortuosity)	0.0001
P(Max Treat Pressure |Poor Erosion)	0.0001	P(Max Treat Pressure |Poor Erosion)	0.0001
P(Reduced Fracture Geometry |Degree of Tortuosity)	0.0001	P(Reduced Fracture Geometry |Degree of Tortuosity)	0.0001
P(Max Treat Pressure |Degree of Tortuosity)	0.0001	P(Max Treat Pressure |Degree of Tortuosity)	0.0001

Table F-2

Sobol's sensitivity analysis results for the Truncated Gaussian Distribution Sampling ($\sigma = 0.1$)

Truncated Gaussian Distribution Ranking - $\sigma = 0.1$			
Parameter	First-order	Parameter	Total order
P(Perforation Friction)	0.3101	P(Perforation Friction)	0.3288
P(NWB Friction)	0.2888	P(NWB Friction)	0.2958
P(Degree of Tortuosity |High Perforation Friction)	0.0963	P(Natural Fissures)	0.0991
P(Natural Fissures)	0.0956	P(Degree of Tortuosity |High NWB Friction)	0.0981
P(Degree of Tortuosity |High NWB Friction)	0.0832	P(Degree of Tortuosity |High Perforation Friction)	0.0968
P(Pad Design)	0.0504	P(High Permeability Zones)	0.0507
P(High Permeability Zones)	0.0445	P(Closure Gradient)	0.0237
P(Closure Gradient)	0.0298	P(Pad Design)	0.0218
P(Fluid Viscosity)	0.0203	P(Reduced Fracture Geometry |Natural Fissures)	0.0146
P(Fluid Efficiency |Excessive Leak-Off)	0.0185	P(Fluid Efficiency |Excessive Leak-Off)	0.0125
P(Reduced Fracture Geometry |Natural Fissures)	0.0022	P(Fluid Viscosity)	0.0081
P(Excessive Leak-Off |High Permeability Zones)	0.0015	P(Excessive Leak-Off |High Permeability Zones)	0.0072
P(Excessive Leak-Off |Natural Fissures)	0.0013	P(Excessive Leak-Off |Natural Fissures)	0.0041
P(Reduced Fracture Geometry |Multiple Fractures)	0.0012	P(Pump Proppant Slugs |Degree of Tortuosity)	0.0039
P(Fluid Efficiency |Low Fluid Viscosity)	0.0011	P(Max Treat Pressure |High Closure Gradient)	0.0015
P(Reduced Fracture Geometry |Pad Design)	0.0011	P(Reduced Fracture Geometry |Pad Design)	0.0006
P(Max Treat Pressure |High Closure Gradient)	0.0011	P(Poor Erosion)	0.0003
P(Pump Proppant Slugs |Degree of Tortuosity)	0.0001	P(Fluid Efficiency |Low Fluid Viscosity)	0.0001
P(Max Treat Pressure |Poor Erosion)	0.0001	P(Max Treat Pressure |Degree of Tortuosity)	0.0001
P(Reduced Fracture Geometry |Degree of Tortuosity)	0.0001	P(Reduced Fracture Geometry |Degree of Tortuosity)	0.0001
P(Poor Erosion)	0.0001	P(Reduced Fracture Geometry |Multiple Fractures)	0.0001
P(Max Treat Pressure |Degree of Tortuosity)	0.0001	P(Max Treat Pressure |Poor Erosion)	0.0001

Table F-3

Sobol's sensitivity analysis results for the Truncated Gaussian Distribution Sampling ($\sigma = 0.15$)

Truncated Gaussian Distribution Ranking - $\sigma = 0.15$			
Parameter	First-order	Parameter	Total order
P(NWB Friction)	0.3181	P(Perforation Friction)	0.3826
P(Perforation Friction)	0.2565	P(NWB Friction)	0.3433
P(Degree of Tortuosity |High Perforation Friction)	0.0929	P(Degree of Tortuosity |High Perforation Friction)	0.1232
P(Natural Fissures)	0.0923	P(Natural Fissures)	0.0997
P(Degree of Tortuosity |High NWB Friction)	0.0803	P(Degree of Tortuosity |High NWB Friction)	0.0993
P(Pad Design)	0.0486	P(Pad Design)	0.0488
P(Closure Gradient)	0.0329	P(High Permeability Zones)	0.0315
P(High Permeability Zones)	0.0304	P(Closure Gradient)	0.0212
P(Reduced Fracture Geometry |Multiple Fractures)	0.0254	P(Fluid Efficiency |Excessive Leak-Off)	0.0158
P(Fluid Viscosity)	0.0178	P(Fluid Viscosity)	0.0119
P(Excessive Leak-Off |High Permeability Zones)	0.0021	P(Reduced Fracture Geometry |Natural Fissures)	0.0058
P(Fluid Efficiency |Low Fluid Viscosity)	0.0014	P(Reduced Fracture Geometry |Multiple Fractures)	0.0056
P(Fluid Efficiency |Excessive Leak-Off)	0.0012	P(Excessive Leak-Off |High Permeability Zones)	0.0051
P(Excessive Leak-Off |Natural Fissures)	0.0011	P(Excessive Leak-Off |Natural Fissures)	0.0047
P(Max Treat Pressure |High Closure Gradient)	0.0011	P(Max Treat Pressure |High Closure Gradient)	0.0018
P(Reduced Fracture Geometry |Natural Fissures)	0.0009	P(Reduced Fracture Geometry |Pad Design)	0.0009
P(Reduced Fracture Geometry |Pad Design)	0.0008	P(Fluid Efficiency |Low Fluid Viscosity)	0.0006
P(Poor Erosion)	0.0001	P(Pump Proppant Slugs |Degree of Tortuosity)	0.0001
P(Max Treat Pressure |Degree of Tortuosity)	0.0001	P(Max Treat Pressure |Poor Erosion)	0.0001
P(Reduced Fracture Geometry |Degree of Tortuosity)	0.0001	P(Reduced Fracture Geometry |Degree of Tortuosity)	0.0001
P(Pump Proppant Slugs |Degree of Tortuosity)	0.0001	P(Max Treat Pressure |Degree of Tortuosity)	0.0001
P(Max Treat Pressure |Poor Erosion)	0.0001	P(Poor Erosion)	0.0001

Table F-4

Sobol's sensitivity analysis results for the Truncated Gaussian Distribution Sampling ($\sigma = 0.2$)

Truncated Gaussian Distribution Ranking - $\sigma = 0.2$			
Parameter	First-order	Parameter	Total order
P(NWB Friction)	0.3064	P(Perforation Friction)	0.3822
P(Perforation Friction)	0.2854	P(NWB Friction)	0.3409
P(Degree of Tortuosity |High Perforation Friction)	0.1199	P(Degree of Tortuosity |High Perforation Friction)	0.1364
P(Natural Fissures)	0.0932	P(Degree of Tortuosity |High NWB Friction)	0.1113
P(Degree of Tortuosity |High NWB Friction)	0.0869	P(Natural Fissures)	0.1104
P(High Permeability Zones)	0.0418	P(Pad Design)	0.0464
P(Closure Gradient)	0.0369	P(High Permeability Zones)	0.0346
P(Pad Design)	0.0332	P(Closure Gradient)	0.0214
P(Fluid Viscosity)	0.0218	P(Fluid Efficiency |Excessive Leak-Off)	0.0158
P(Fluid Efficiency |Excessive Leak-Off)	0.0153	P(Fluid Viscosity)	0.0121
P(Excessive Leak-Off |High Permeability Zones)	0.0019	P(Excessive Leak-Off |Natural Fissures)	0.0061
P(Reduced Fracture Geometry |Natural Fissures)	0.0019	P(Reduced Fracture Geometry |Natural Fissures)	0.0059
P(Excessive Leak-Off |Natural Fissures)	0.0018	P(Excessive Leak-Off |High Permeability Zones)	0.0058
P(Reduced Fracture Geometry |Multiple Fractures)	0.0017	P(Reduced Fracture Geometry |Multiple Fractures)	0.0057
P(Max Treat Pressure |High Closure Gradient)	0.0012	P(Max Treat Pressure |High Closure Gradient)	0.0026
P(Reduced Fracture Geometry |Pad Design)	0.0011	P(Reduced Fracture Geometry |Pad Design)	0.0013
P(Fluid Efficiency |Low Fluid Viscosity)	0.0009	P(Fluid Efficiency |Low Fluid Viscosity)	0.0009
P(Pump Proppant Slugs |Degree of Tortuosity)	0.0001	P(Pump Proppant Slugs |Degree of Tortuosity)	0.0001
P(Max Treat Pressure |Poor Erosion)	0.0001	P(Max Treat Pressure |Poor Erosion)	0.0001
P(Reduced Fracture Geometry |Degree of Tortuosity)	0.0001	P(Reduced Fracture Geometry |Degree of Tortuosity)	0.0001
P(Poor Erosion)	0.0001	P(Max Treat Pressure |Degree of Tortuosity)	0.0001
P(Max Treat Pressure |Degree of Tortuosity)	0.0001	P(Poor Erosion)	0.0001

Table F-5

Sobol's sensitivity analysis results for the Log-odds Distribution Sampling ($\sigma = 0.1$)

Log-odds Distribution Ranking - $\sigma = 0.1$			
Parameter	First-order	Parameter	Total order
P(NWB Friction)	0.3163	P(NWB Friction)	0.3264
P(Perforation Friction)	0.2672	P(Perforation Friction)	0.2721
P(Natural Fissures)	0.1041	P(Degree of Tortuosity |High NWB Friction)	0.0988
P(Degree of Tortuosity |High NWB Friction)	0.0952	P(Natural Fissures)	0.0859
P(Degree of Tortuosity |High Perforation Friction)	0.0806	P(Degree of Tortuosity |High Perforation Friction)	0.0819
P(High Permeability Zones)	0.0311	P(High Permeability Zones)	0.0323
P(Closure Gradient)	0.0291	P(Pad Design)	0.0246
P(Excessive Leak-Off |High Permeability Zones)	0.0242	P(Fluid efficiency |Excessive Leak-Off)	0.0127
P(Pad Design)	0.0144	P(Closure Gradient)	0.0065
P(Fluid efficiency |Excessive Leak-Off)	0.0107	P(Reduced Fracture Geometry |Natural Fissures)	0.0063
P(Reduced Fracture Geometry |Multiple Fractures)	0.0072	P(Fluid Viscosity)	0.0048
P(Fluid Viscosity)	0.0072	P(Reduced Fracture Geometry |Multiple Fractures)	0.0037
P(Reduced Fracture Geometry |Natural Fissures)	0.0053	P(Excessive Leak-Off |High Permeability Zones)	0.0035
P(Excessive Leak-Off |Natural Fissures)	0.0012	P(Excessive Leak-Off |Natural Fissures)	0.0012
P(Max Treat Pressure |High Closure Gradient)	0.0009	P(Max Treat Pressure |High Closure Gradient)	0.0005
P(Reduced Fracture Geometry |Pad Design)	0.0003	P(Fluid efficiency |Low Fluid Viscosity)	0.0002
P(Fluid efficiency |Low Fluid Viscosity)	0.0002	P(Pump proppant slugs |Degree of Tortuosity)	0.0001
P(Pump proppant slugs |Degree of Tortuosity)	0.0001	P(Max Treat Pressure |Poor Erosion)	0.0001
P(Max Treat Pressure |Poor Erosion)	0.0001	P(Poor Erosion)	0.0001
P(Poor Erosion)	0.0001	P(Reduced Fracture Geometry |Degree of Tortuosity)	0.0001
P(Reduced Fracture Geometry |Degree of Tortuosity)	0.0001	P(Max Treat Pressure |Degree of Tortuosity)	0.0001
P(Max Treat Pressure |Degree of Tortuosity)	0.0001	P(Reduced Fracture Geometry |Pad Design)	0.0001

Table F-6

Sobol's sensitivity analysis results for the Log-odds Distribution Sampling ($\sigma = 0.15$)

Log-odds Distribution Ranking - $\sigma = 0.15$			
Parameter	First-order	Parameter	Total order
P(Perforation Friction)	0.3275	P(Perforation Friction)	0.3277
P(NWB Friction)	0.2906	P(NWB Friction)	0.2912
P(Degree of Tortuosity |High Perforation Friction)	0.1017	P(Natural Fissures)	0.1541
P(Degree of Tortuosity |High NWB Friction)	0.0982	P(Degree of Tortuosity |High Perforation Friction)	0.1395
P(Natural Fissures)	0.0823	P(Degree of Tortuosity |High NWB Friction)	0.1082
P(High Permeability Zones)	0.0299	P(Pad Design)	0.0332
P(Pad Design)	0.0212	P(High Permeability Zones)	0.0303
P(Fluid efficiency |Excessive Leak-Off)	0.0206	P(Fluid efficiency |Excessive Leak-Off)	0.0126
P(Excessive Leak-Off |High Permeability Zones)	0.0178	P(Closure Gradient)	0.0082
P(Fluid Viscosity)	0.0173	P(Reduced Fracture Geometry |Natural Fissures)	0.0071
P(Reduced Fracture Geometry |Multiple Fractures)	0.0044	P(Fluid Viscosity)	0.0052
P(Reduced Fracture Geometry |Natural Fissures)	0.0023	P(Excessive Leak-Off |High Permeability Zones)	0.0047
P(Closure Gradient)	0.0018	P(Reduced Fracture Geometry |Pad Design)	0.0045
P(Excessive Leak-Off |Natural Fissures)	0.0013	P(Excessive Leak-Off |Natural Fissures)	0.0012
P(Fluid efficiency |Low Fluid Viscosity)	0.0009	P(Reduced Fracture Geometry |Multiple Fractures)	0.0006
P(Reduced Fracture Geometry |Pad Design)	0.0008	P(Fluid efficiency |Low Fluid Viscosity)	0.0003
P(Max Treat Pressure |High Closure Gradient)	0.0006	P(Reduced Fracture Geometry |Degree of Tortuosity)	0.0002
P(Pump proppant slugs |Degree of Tortuosity)	0.0001	P(Pump proppant slugs |Degree of Tortuosity)	0.0001
P(Max Treat Pressure |Poor Erosion)	0.0001	P(Max Treat Pressure |Poor Erosion)	0.0001
P(Poor Erosion)	0.0001	P(Poor Erosion)	0.0001
P(Reduced Fracture Geometry |Degree of Tortuosity)	0.0001	P(Max Treat Pressure |Degree of Tortuosity)	0.0001
P(Max Treat Pressure |Degree of Tortuosity)	0.0001	P(Max Treat Pressure |High Closure Gradient)	0.0001

Table F-7

Sobol's sensitivity analysis results for the Log-odds Distribution Sampling ($\sigma = 0.2$)

Log-odds Distribution Ranking - $\sigma = 0.2$			
Parameter	First-order	Parameter	Total order
P(Perforation Friction)	0.3223	P(Perforation Friction)	0.3275
P(NWB Friction)	0.2844	P(NWB Friction)	0.2877
P(Degree of Tortuosity |High Perforation Friction)	0.1031	P(Natural Fissures)	0.1163
P(Degree of Tortuosity |High NWB Friction)	0.0932	P(Degree of Tortuosity |High Perforation Friction)	0.1088
P(Natural Fissures)	0.0834	P(Degree of Tortuosity |High NWB Friction)	0.0984
P(Closure Gradient)	0.0335	P(Pad Design)	0.0348
P(Pad Design)	0.0233	P(High Permeability Zones)	0.0313
P(Fluid efficiency |Excessive Leak-Off)	0.0232	P(Fluid efficiency |Excessive Leak-Off)	0.0128
P(High Permeability Zones)	0.0213	P(Closure Gradient)	0.0092
P(Reduced Fracture Geometry |Natural Fissures)	0.0113	P(Reduced Fracture Geometry |Natural Fissures)	0.0074
P(Fluid Viscosity)	0.0031	P(Fluid Viscosity)	0.0057
P(Excessive Leak-Off |High Permeability Zones)	0.0026	P(Excessive Leak-Off |High Permeability Zones)	0.0055
P(Reduced Fracture Geometry |Multiple Fractures)	0.0025	P(Reduced Fracture Geometry |Multiple Fractures)	0.0046
P(Excessive Leak-Off |Natural Fissures)	0.0009	P(Excessive Leak-Off |Natural Fissures)	0.0014
P(Fluid efficiency |Low Fluid Viscosity)	0.0008	P(Max Treat Pressure |High Closure Gradient)	0.0007
P(Max Treat Pressure |High Closure Gradient)	0.0008	P(Reduced Fracture Geometry |Pad Design)	0.0003
P(Reduced Fracture Geometry |Pad Design)	0.0006	P(Fluid efficiency |Low Fluid Viscosity)	0.0003
P(Pump proppant slugs |Degree of Tortuosity)	0.0001	P(Pump proppant slugs |Degree of Tortuosity)	0.0001
P(Max Treat Pressure |Poor Erosion)	0.0001	P(Poor Erosion)	0.0001
P(Reduced Fracture Geometry |Degree of Tortuosity)	0.0001	P(Max Treat Pressure |Poor Erosion)	0.0001
P(Poor Erosion)	0.0001	P(Max Treat Pressure |Degree of Tortuosity)	0.0001
P(Max Treat Pressure |Degree of Tortuosity)	0.0001	P(Reduced Fracture Geometry |Degree of Tortuosity)	0.0001

14. Appendix G

In summary, in this work the following methods have been used:

1. Bayesian Belief Network
2. Weighted Sum Algorithm (Experts Judgement Elicitation method)
3. Log-likelihood method (Experts Judgement Elicitation method)
4. Elicitation method for Bayesian Belief Network (Experts Judgement Elicitation method)
5. Sensitivity Analysis
6. Sobol's Variance Decomposition method (Sensitivity Analysis)
7. Uncertainty Analysis
8. Risk Importance Measures Analysis
9. Cost-Benefit Analysis

15. References

[1] D. Valis, M. Koucky, "Selected Overview of Risk Assessment Techniques", ISSN 1232-9312, 4-2009, p. 19-32, DOI: bwmeta1.element.baztech-article-BAR0-0046-0019, 2009.

[2] F. Jahn, M. Cook, M. Graham, "Hydrocarbon Exploration and Production", Series on Developments in Petroleum Science: Volume 55, 2nd Edition, 2008.

[3] E. Zio, "An Introduction to the Basics of Reliability and Risk Analysis", Series on Quality, Reliability and Engineering Statistics: Vol.13, World Scientific, 2007.

[4] A. Tatomir, C. Mcdermott, J. Bensabat, H. Class, K. Edlmann, R. Taherdangkoo, And M. Sauter, "Conceptual Model Development Using A Generic Features, Events And Processes (FEP) Database for Assessing the Potential Impact of Hydraulic Fracturing on Groundwater Aquifers", Advances in Geosciences 45:185-192, DOI: 10.5194/adgeo-45-185-2018, 2018.

[5] X. Cai, B. Guo, "Semi Analytical Model for Predicting Screenout In Hydraulic Fracturing in Vertical Wells", Journal of Natural Gas Science and Engineering, Volume 52, April 2018, Pages 117-127, doi.org/10.1016/j.jngse.2017.12.028.

[6] M. Economides, T. Martin, "Modern Fracturing", ET Publishing, 2007, Chapter 5.

[7] M. Economides, K. Nolte, "Reservoir Stimulation", Third Edition, 2000, Chapters 5-6.

[8] C. Lu, M. Li1, J. Guo1, X. Tang, H. Zhu, W. Yong-Hui, H. Liang, "Engineering Geological Characteristics and The Hydraulic Fracture Propagation Mechanism of The Sand-Shale Interbedded Formation in The Xu5 Reservoir", Journal of Geophysics and Engineering 12(3), DOI: 10.1088/1742-2132/12/3/321, 2015.

[9] E. Zio, A. Salo, E. Tosoni, "Measures of Risk Importance for Probabilistic Scenario Analysis", manuscript submitted for publication, 2019.

[10] E. Zio, E. Tosoni, A. Salo, J. Govaerts, "Comprehensiveness of Scenarios in the Safety Assessment of Nuclear Waste Repositories", Reliability Engineering & System Safety, 188 (2019) 561-573.

[11] X. Weng, "Modeling of complex hydraulic fractures in naturally fractured formation", Journal of Unconventional Oil and Gas Resources, Volume 9, March 2015, Pages 114-135 2015, doi.org/10.1016/j.juogr.2014.07.001.

[12] F. Hansson, S. Sjokvist, “Modelling Expert Judgement into a Bayesian Belief Network: a Method for Consistent and Robust Determination of Conditional Probability Tables”, Lund University, 2013:E37.

[13] J. Nunes, M. Barbosa, L. Silva, K. Gorgônio, H. Almeida, A. Perkusich, “Issues in the Probability Elicitation Process of Expert-Based Bayesian Networks”, Enhanced Expert Systems, DOI: 10.5772/intechopen.81602, 2018.

[14] S. Baker, E. Mendes, “Evaluating the Weighted Sum Algorithm for Estimating Conditional Probabilities in Bayesian Networks”, Proceedings of the 22nd International Conference on Software Engineering & Knowledge Engineering (SEKE'2010), 2010.

[15] E. Kemp-Benedict, “Elicitation Techniques for Bayesian Network Models”, Stockholm Environment Institute, Working Paper WP-US-0804, 2008.

[16] E. Zio, “Computational Methods for Reliability and Risk Analysis”, Series on Quality, Reliability and Engineering Statistics: Volume 14, doi.org/10.1142/7190, 2009.

[17] I.M. Sobol’, “Global sensitivity indices for nonlinear mathematical models and their Monte Carlo estimates”, Mathematics and Computers in Simulation: Volume 55, Issues 1–3, 15 February 2001, Pages 271-280, doi.org/10.1016/S0378-4754(00)00270-6.

[18] J. Morio, “Global and local sensitivity analysis methods for a physical system”, European Journal of Physics 32(6):1577, DOI: 10.1088/0143-0807/32/6/011, 2011.

[19] Z. Hu, “Probability Models for Data-Driven Global Sensitivity Analysis”, Reliability Engineering & System Safety, DOI: 10.1016/j.ress.2018.12.003, 2018.

[20] L. C. van der Gaag, R. Kuijper, Y. M. van Geffen, J. L. Vermeulen, “Towards Uncertainty Analysis of Bayesian Networks”, 25th Benelux Conference on Artificial Intelligence, 2013.

[21] M. Pradhan, K. Huang, B.D. Favero, M. Henrion, G. Provan, “The Sensitivity of Belief Networks to imprecise probabilities: an Experimental Investigation”, Artificial Intelligence, Volume 85, Issues 1–2, August 1996, Pages 363-397, doi.org/10.1016/0004-3702(96)00002-1.

[22] H. Wang, “Building Bayesian Networks: elicitation, evaluation, and learning”, University of Pittsburgh, 2004.

[23] J. Rohmer, P. Gehl, “Sensitivity analysis of Bayesian networks to parameters of the conditional probability model using a Beta regression approach”, Expert Systems with Applications: Volume 145, 113130, doi.org/10.1016/j.eswa.2019.113130, 2019.

[24] C. Li, “Sensitivity Analysis and Uncertainty Integration for System Diagnosis and Prognosis”, Vanderbilt University, 2016.

[25] C. Li, S. Mahadevan, “Sensitivity Analysis of a Bayesian Network”, DOI: 10.1115/1.4037454, 2017.

[26] M. Pradhan, M. Henrion, G. Provan, B. Del Favero, K. Huang, “Intelligence The sensitivity of belief networks to imprecise probabilities: an experimental investigation”, Artificial Intelligence: Volume 85, Issues 1–2, August 1996, Pages 363-397, doi.org/10.1016/0004-3702(96)00002-1.

[27] K. Murphy, “Bayes Net Toolbox for Matlab”, Computing Science and Statistics, 33, 1024-1034, 2001.

[28] M. Leimeister, A. Kolios, “A review of reliability-based methods for risk analysis and their application in the offshore wind industry”, Renewable and Sustainable Energy Reviews, Volume 91, Pages 1065-107, https://doi.org/10.1016/j.rser.2018.04.004, 2018.

[29] G. Song, F. Khan, H. Wang, S. Leighton, Z. Yuan, H. Liu, “Dynamic occupational risk model for offshore operations in harsh environments”, Reliability Engineering & System Safety, Volume 150, Pages 58-64, https://doi.org/10.1016/j.ress.2016.01.021, 2016.

[30] M. L. Fam, X. He, D. Konovessis, L. S. Ong, “Using Dynamic Bayesian Belief Network for analysing well decommissioning failures and long-term monitoring of decommissioned wells”, Reliability Engineering & System Safety, Volume 197, 106855, https://doi.org/10.1016/j.ress.2020.106855, 2020.

[31] I. Animah, M. Shafiee, “Application of risk analysis in the liquefied natural gas (LNG) sector: An overview”, Journal of Loss Prevention in the Process Industries, Volume 63, https://doi.org/10.1016/j.jlp.2019.103980, 2020.

[32] F. I.Khan, P. R. Amyotte, Md. T. Amin, “Chapter One - Advanced methods of risk assessment and management: An overview”, Methods in Chemical Process Safety, Volume 4, Pages 1-34, https://doi.org/10.1016/bs.mcps.2020.03.002, 2020.

[33] B. G. Marcot, J. D. Steventon, G. D. Sutherland, and R. K. McCann, “Guidelines for developing and updating Bayesian belief networks applied to ecological modeling and conservation”, Canadian Journal of Forest Research 36(12), DOI: 10.1139/x06-135, 2006.

[34] N. Bilal, “Implementation of Sobol’s Method of Global Sensitivity Analysis to a Compressor Simulation Model”, International Compressor Engineering Conference, 2014.